https://doi.org/10.5194/gmd-2020-205
Preprint. Discussion started: 24 July 2020

Geoscientific Model Development Discussions

Manuscript prepared for Geosci. Model Dev.
with version 2014/09/16 7.15 Copernicus papers of the LaTeX class copernicus.cls.
Date: 23 July 2020

JULES-CN: a coupled terrestrial Carbon-Nitrogen Scheme (JULES vn5.1)

Andrew J. Wiltshire[1,2], Eleanor J. Burke[1], Sarah E. Chadburn[3], Chris D. Jones[1], Peter M. Cox[3], Taraka Davies-Barnard[3], Pierre Friedlingstein[3], Anna B. Harper[3], Spencer Liddicoat[1], Stephen Sitch[2], and Sönke Zaehle[4]

[1]Met Office Hadley Centre, Exeter, Devon, UK EX1 3PB
[2]College of Life and Environmental Sciences, University of Exeter, Exeter, EX4 4RJ
[3]College of Engineering, Mathematics, and Physical Sciences, University of Exeter, Exeter, EX4 4QE
[4]Biogeochemical Signals Department, Max Planck Institute for Biogeochemistry, 07745 Jena, Germany

Correspondence to: Andrew Wiltshire (andy.wiltshire@metoffice.gov.uk)

Abstract. Understanding future changes in the terrestrial carbon cycle is important for reliable projections of climate change and impacts on ecosystems. It is known that nitrogen could limit plants' response to increased atmospheric carbon dioxide and is therefore important to include in Earth System Models. Here we present the implementation of the terrestrial nitrogen cycle in the JULES land surface model (JULES-CN). Two versions are discussed - the one implemented within the UK Earth System Model (UKESM1) which has a bulk soil biogeochemical model and a development version which resolves the soil biogeochemistry with depth. The nitrogen cycle is based on the existing carbon cycle in the model. It represents all the key terrestrial nitrogen processes in an efficient way. Biological fixation and nitrogen deposition are external inputs, and loss occurs via leaching and a bulk gas loss parameterisation. Nutrient limitation reduces carbon-use efficiency (CUE - ratio of net to gross primary productivity) and can slow soil decomposition. We show that ecosystem level limitation of net primary productivity by nitrogen is consistent with observational estimates and that simulated carbon and nitrogen pools and fluxes are comparable to the limited available observations. The impact of N limitation is most pronounced in northern mid-latitudes. The introduction of a nitrogen cycle improves the representation of interannual variability of global net ecosystem exchange which was much too pronounced in the carbon cycle only versions of JULES (JULES-C). It also reduces the CUE and alters its response over the twentieth century and limits the CO_2-fertilisation effect, such that the simulated current day land carbon sink is reduced by about 0.5 Pg C yr^{-1}. The inclusion of a prognostic land nitrogen scheme marks a step forward in functionality and realism for the JULES and UKESM models.

https://doi.org/10.5194/gmd-2020-205
Preprint. Discussion started: 24 July 2020

Geoscientific Model Development Discussions
Open Access
EGU

1 Introduction

Terrestrial ecosystems absorb around 25% of anthropogenic carbon emissions (Le Quéré et al., 2018; Friedlingstein et al., 2019), and changes in the future land carbon sink will feedback to climate via the proportion of the emissions remaining in the atmosphere. Under projected climate change, the primary mechanism for increased terrestrial sequestration is an increase in plant productivity and biomass, which relies on sufficient availability of nitrogen within the soil-plant system. Therefore the availability of nitrogen impacts the land carbon sink, both in the present and in a higher atmospheric carbon dioxide (CO_2) future.

Nitrogen exists in the terrestrial system in organic and inorganic forms and is continually cycled. In a stable climate the external inputs–biological fixation and nitrogen deposition –are balanced by the external losses–leaching and gas loss. Depending on the nutrient status of the vegetation and soil, changes in the balance of the inputs and outputs of nitrogen can drive adjustments in vegetation biomass and soil organic matter. Internally organic nitrogen is lost from vegetation through the production of litter and disturbance. The litter decomposes into soil organic matter and in turn is mineralised into inorganic nitrogen. Both inorganic and organic nitrogen may become available for plant uptake (Weintraub and Schimel, 2005).

In a changing climate, rising atmospheric CO_2 drives an increase in the terrestrial carbon cycle and Gross Primary Productivity (GPP). This extra demand for nitrogen will limit the potential increase in future carbon stocks. For example, Zaehle (2013a) suggest that, in some areas, nitrogen could limit future carbon uptake by up to 70%. Nitrogen cycling also tends to reduce the sensitivity of land carbon uptake to temperature. Warmer conditions lead to increased plant respiration and soil respiration, which tends to reduce the land carbon sink. However, the increased soil respiration also leads to accelerated nitrogen mineralisation and increased nitrogen availability to plants, which may provide a counteracting increase in GPP. This latter effect is absent from models that do not include a nitrogen cycle, As a result of neglecting these important effects, land-surface models without an interactive nitrogen cycle tend to overestimate both CO_2 and temperature effects on the land carbon sink (Wenzel et al., 2016; Cox et al., 2013). An increasing number of land surface and climate models now include constraints on the land carbon sink caused by nitrogen limitation (Zaehle et al., 2014; Wania et al., 2012; Smith et al., 2014). Recent simulations have generated a range of estimates for the sensitivity of the C cycle to N availability (Meyerholt et al., 2020a; Davies-Barnard et al., 2020; Arora et al., 2019). For example, Meyerholt et al. (2020a) use a perturbed model ensemble and show that the projected future increase in land carbon store caused by CO_2 fertilisation is reduced by between 9 and 39 % due to nitrogen limitation and the projected losses in terrestrial carbon caused by climate change are between a reduction of 39 % and a slight increase of 1 %.

https://doi.org/10.5194/gmd-2020-205
Preprint. Discussion started: 24 July 2020

The purpose of this paper is to describe and evaluate the implementation of a coupled carbon and nitrogen cycle within the Joint UK Land-Environment Simulator (Best et al., 2011; Clark et al., 2011) (JULES at vn5.1 - http://jules-lsm.github.io/vn5.1/release_notes/JULES5.1.html). JULES is the land surface component of the later generation of Hadley Centre climate models including the UK Earth System Model (UKESM) (Sellar et al., 2019). The addition of the nitrogen component described here was carried out alongside other developments such as improved plant physiology and extended plant functional types (Harper et al., 2018), an enhanced representation of surface exchange and hydrology (Wiltshire et al., 2020) and a new managed land module (Robertson and Liddicoat, in prep.). These separate components have been combined to make the land surface component of UKESM and were used for the most recent Global Carbon Budget annual assessment (Friedlingstein et al., 2019).

The philosophy behind the developments described here is to produce a parsimonious model that captures the large-scale role of nitrogen limitation on carbon use efficiency (CUE - ratio of net to gross primary productivity) and net ecosystem productivity (NEP). This is achieved by extending the implicit representation of nitrogen in the existing dynamic vegetation and plant physiology modules to enable a more comprehensive nitrogen cycle within the land surface. Nutrient limitation operates through two mechanisms; the available carbon for growth and spreading is reduced, and the decomposition of litter carbon into the soil carbon is slowed. This is achieved by explicitly representing the demand for nitrogen within the vegetation and soil modules and then reducing plant net carbon gain to match available nutrients. In the soil module an additional decomposition rate modifier is introduced that slows decomposition to match available nutrients. The current structure of the TRIFFID dynamic vegetation model (Cox, 2001), in particular the fixed allometry and carbon allocation, is largely unchanged. As the aim of this scheme is to capture the impact on terrestrial carbon stores, loss terms are aggregated and not speciated. The model's reduction of vegetation growth and spreading due to nitrogen limitation will have only a minor impact on the GPP and autotrophic respiration. Therefore the emergent impact of the nitrogen scheme will be to reduce NPP and hence the carbon use efficiency of the vegetation. The excess carbon which cannot be used for growth goes to non structural carbohydrates, root exudates and biogenic volatile organic compounds (Collalti and Prentice, 2019).

Two nitrogen model configurations are described here–JULES-CN and JULES-CN$_{layered}$–both of which are directly derived from the JULES-C configuration. JULES-C is the land configuration of the HadGEM2-ES (Collins et al., 2011) Earth System Model used in CMIP5 (Taylor et al., 2012), and is also used in the Global Carbon Budget annual assessments (Le Quéré et al., 2018) coupled carbon-nitrogen model based on JULES-C. The soil biogeochemistry is represented by a single level in JULES-CN whereas it varies as a function of depth in JULES-CN$_{layered}$. This paper describes

https://doi.org/10.5194/gmd-2020-205
Preprint. Discussion started: 24 July 2020


Geoscientific Model Development Discussions

the additional model structure required for the two configurations; and assesses the simulated stocks and fluxes and their changes over the 20^{th} century.

2 JULES model description

JULES is the land surface component of the new UK community Earth System model, UKESM1 (Sellar et al., 2019). JULES can also be run offline forced by observed meteorology globally, regionally or at a single location. A full description of JULES is provided by Best et al. (2011) and Clark et al. (2011). In particular, JULES represents the surface energy balance, a dynamic snowpack model (one dimensional), vertical heat and water fluxes, soil freezing, large scale hydrology, and carbon fluxes and storage in both vegetation and soil. Within JULES, carbon dynamics in soils and vegetation and dynamic vegetation are provided by Top-Down Representation of Interactive Foliage and Flora Including Dynamics (TRIFFID) (Cox, 2001). In this version of TRIFFID, five plant functional types (PFTs) are included: broadleaf tree, needleleaf tree, C_3 grasses, C_4 grasses and shrubs. The soil carbon model in JULES-C is based on the RothC model (Clark et al., 2011). Recently, Burke et al. (2017); Chadburn et al. (2015) added a representation of permafrost soil processes to JULES, including a representation of the vertical distribution of soil carbon which we build upon here.

3 Model developments

What follows is a description of the extension of the carbon cycle used by JULES-C in HadGEM2-ES (Collins et al., 2011) and Global Carbon Budget annual assessment in 2018 (Le Quéré et al., 2018) to include an interactive nitrogen cycle. As standard, JULES-C includes an implicit representation of nitrogen which has been extended to be fully interactive. For clarity we include a full description including the existing TRIFFID and RothC models and highlight where and how they have been extended.

The nitrogen model is included within the TRIFFID dynamic vegetation and RothC soil carbon models. The vegetation nitrogen component captures the nitrogen limitation on the C stock, and includes retranslocation and the presence of a labile N pool per PFT (Figure 1). The vegetation uptakes nitrogen from the inorganic nitrogen pool. In JULES-CN one inorganic nitrogen pool is shared between all of the different PFTs irrespective of their rooting profile. However, in the multi-layered soil biogeochemistry model (JULES-CN$_{layered}$), the availability of inorganic nitrogen depends on the distribution of the plant roots. The soil nitrogen component simulates mineralisation and immobilisation, and during any periods of nitrogen limitation it slows the rate of litter decomposition into

https://doi.org/10.5194/gmd-2020-205
Preprint. Discussion started: 24 July 2020


Geoscientific Model Development Discussions

soil organic matter.

JULES-CN requires 7 new parameters (leaf and root retranslocation, the coefficient of fixation, inorganic nitrogen turnover, soil C:N ratios, a gas emission scalar and the effective solubility of nitrogen), 3 prognostics (organic nitrogen pools of decomposable and resistant plant material and an inorganic nitrogen pool) and 3 diagnostic nitrogen pools (plant labile nitrogen, and organic nitrogen pools of humified soil and microbial biomass). JULES-CN$_{layered}$ additionally includes the plant available fraction of the inorganic nitrogen pool and a diffusion term to transfer the inorganic nitrogen from plant-unavailable to plant-available.

3.1 Vegetation carbon and nitrogen

At the core of the vegetation model is the TRIFFID Dynamic vegetation model (Cox, 2001). TRIFFID represents the vegetation cover at each location in terms of the fractional area covered, and the leaf area index and canopy height of each PFT. The mean canopy height is converted via allometric equations into a maximum or *balanced leaf area index* ($\mathcal{L}_b$) for each PFT. The vegetation carbon density per PFT (C_v) can be separated into leaf (L_c), root (R_c) and total stem (W_c) pools, each of which is related allometrically to $\mathcal{L}_b$:

$$C_v = L_c + R_c + W_c \tag{1}$$

$$L_c = \sigma_l \mathcal{L}_b \tag{2}$$

$$R_c = L_c \tag{3}$$

$$W_c = a_{wl}(L_b)^{b_{wl}} \tag{4}$$

Where σ_l, a_{wl} and b_{wl} are PFT dependent allometric parameters (Table 1). By definition $\mathcal{L}_b$ does not have an explicit seasonal cycle but responds to changes in the vegetation carbon on both short (seasonal) and long (centennial) timescales. [It should be noted that leaf seasonality is represented by a separate phenology model.] A high $\mathcal{L}_b$ is related to a high carbon density and canopy height. The canopy height (h) is defined allometrically by:

$$h = \frac{W_c}{a_{wl}\eta_{sl}} \left(\frac{a_{wl}}{W_c}\right)^{1/b_{wl}} \tag{5}$$

https://doi.org/10.5194/gmd-2020-205
Preprint. Discussion started: 24 July 2020


Geoscientific Model Development Discussions

where η_{sl} relates respiring stem to leaf carbon (Table 1). We can combine equations 4 and 5 to relate ($\mathcal{L}_b$) to canopy height (h) and these two variables can be used interchangeably to describe the state of the vegetation.

The root and total stem nitrogen pools are defined using stoichiometric relationships as a function of the carbon pools. These stoichiometric functions already exist in the model and are used in the calculation of plant maintenance respiration. We extend their use to explicitly define nitrogen pools as part of the new scheme.

$$R_n = \mu_{rl}\, n_{l0}\, R_c \tag{6}$$

$$W_n = \mu_{sl}\, n_{l0}\, W_c \tag{7}$$

where μ_{rl} and μ_{sl} are stoichiometric parameters linking the top leaf nitrogen concentration (n_{l0}) to the total stem and root nitrogen pools (W_n and R_n, respectively). The leaf nitrogen pool (L_n) has an additional dependency on phenological state (3.1.2) and assumed distribution of nitrogen in the canopy (3.1.3). Following Equation 1 the total vegetation nitrogen store per PFT is given by:

$$N_v = L_n + R_n + W_n \tag{8}$$

The C:N ratio of the root and stem pools are constant in time and leaf pool C:N ratio only varies with phenological state. However, the relative proportions of each pool vary with total biomass resulting in the whole plant C:N ratio increasing with total vegetation carbon (Fig. 2). This is due to the relatively greater proportion of stem carbon at higher biomass. Therefore woody vegetation has the highest C:N ratios due to the greater proportion of stem wood in comparison to grasses. The total vegetation nitrogen increases with canopy height (Fig. 3).

3.1.1 Biological Nitrogen Fixation

Biological nitrogen fixation (BNF) is assumed to be the largest supplier of nitrogen to the terrestrial ecosystem. Following Cleveland et al. (1999), the nitrogen fixation is determined as a proportion of the net primary production before nitrogen limitation (NPP_{pot}).

$$F = \zeta NPP_{pot} \tag{9}$$

The rate of fixation (ζ) is set such that global present day net primary productivity of approximately 60 Pg C yr^{-1} results in approximately 100 Tg N yr^{-1} fixation (0.0016 kg N kg C $^{-1}$), within the range most recent global estimate of BNF (Davies-Barnard and Friedlingstein, 2020). In JULES-CN this fixation is directly transferred into the inorganic soil nitrogen pool and becomes available as

https://doi.org/10.5194/gmd-2020-205
Preprint. Discussion started: 24 July 2020

Geoscientific Model Development Discussions
Open Access
EGU

Table 1. Default values of PFT-specific parameters for allometry, allocation and vegetation nitrogen and carbon stoichiometry in the JULES-CN and JULES-CN$_{layered}$ configurations.

		Broadleaf tree	Needleleaf tree	C_3 grass	C_4 grass	Shrub
a_{wl} (kg [C] m^{-2})	Allometric coefficient	0.65	0.65	0.005	0.005	0.10
a_{ws}	Ratio of total to respiring stem carbon	10.00	10.00	1.00	1.00	10.00
b_{wl}	Allometric exponent	1.667	1.667	1.667	1.667	1.667
η_{sl} (kg [C] m^{-2} per unit LAI)	Live stemwood coefficient	0.01	0.01	0.01	0.01	0.01
μ_{rl} (-)	Ratio of root to top leaf nitrogen	1.00	1.00	1.00	1.00	1.00
μ_{sl} (-)	Ratio of stem to top leaf nitrogen	0.10	0.10	1.00	1.00	0.10
n_{l0} (kg [N])(kg [C])$^{-1}$)	Top leaf nitrogen concentration	0.046	0.033	0.073	0.060	0.060
k_n	nitrogen profile coefficient	0.78	0.78	0.78	0.78	0.78
λ_r	root nitrogen retranslocation coefficient	0.2	0.2	0.2	0.2	0.2
λ_l	leaf nitrogen retranslocation coefficient	0.5	0.5	0.5	0.5	0.5
$\mathcal{L}_{min}$	Minimum balanced leaf area index	3.0	3.0	1.0	1.0	1.0
$\mathcal{L}_{max}$	Maximum balanced leaf area index	9.0	9.0	4.0	4.0	4.0
n_{l0} (kg [N])(kg [C])$^{-1}$)	Top leaf nitrogen concentration	0.046	0.033	0.073	0.060	0.060

inorganic nitrogen. However, in JULES-CN$_{layered}$ the vertical distribution of the fixed nitrogen in the soil depends on the root distribution and the freeze/thawed status (being distributed proportionally to the fraction of roots in each layer, discounting any frozen layers). If the whole soil is frozen, fixed nitrogen goes into the inorganic nitrogen pool in the top layer. This parameterisation results in a latitudinal gradient with the highest rates of fixation in the tropics and lowest in boreal forests and arctic tundra which is consistent with some estimates of BNF (Houlton et al., 2008) though not recent observation meta-analyses (Davies-Barnard and Friedlingstein, 2020).

3.1.2 Phenology and Mobilisation

The leaf carbon pool (L_c, Equation 2) varies allometrically with the vegetation carbon state on both short (seasonal) and long (centennial) timescales but not with changes in phenological state. Implicit within TRIFFID is a labile leaf carbon pool that acts as a reserve of carbon during spring and a store during fall. L_c is therefore the sum of a labile pool from which carbon can be mobilised during leaf out plus an allocated pool representing the actual leaf area index. The labile pool is zero at full leaf out and at the allometrically defined maximum during the no leaf period. This distinction is inconsequential in the carbon only mode but is more critical when considering nitrogen interactions as the implication is that at all times the plant has enough nitrogen in reserve to maintain full leaf.

https://doi.org/10.5194/gmd-2020-205
Preprint. Discussion started: 24 July 2020


Geoscientific Model Development Discussions
Open Access
EGU

We therefore a new parameterisation of retranslocation and labile nitrogen that is dependent on the phenological state. Leaf phenology is controlled by a second state variable (p) which relates the leaf area index at any moment in time to the balanced leaf area index ($\mathcal{L}_b$).

$$\mathcal{L} = p\mathcal{L}_b \tag{10}$$

where p is a scalar between 0 and 1 that describes the phenological state of the system (Clark et al., 2011). For evergreen plants p is a constant of 1. The two state variables $\mathcal{L}_b$ and p combine to define the vegetation state.

Using the phenological state we extend the equivalent approach to leaf carbon to include the role of retranslocation of nitrogen from the leaves during leaf fall. The leaf nitrogen pool is the sum of allocated and labile components with additional dependencies on the distribution of nitrogen in the canopy and phenological state. This means that the stochiometry of the allocated and labile components are different. During leaf-off the labile component is the equivalent of the retranslocated leaf nitrogen plus an additional store of nitrogen in preparation for the following bud burst. Higher retranslocation implies a larger labile nitrogen store. L_n therefore becomes:

$$L_n = pn_{lc}L_c + (1-p)(\frac{1+\lambda_l}{2})n_{lc}L_c \tag{11}$$

where λ_l is the leaf nitrogen retranslocation coefficient and n_{lc} is the mean canopy nitrogen content (Eq 12). In this configuration λ_l is set to 0.5 for all PFTs (Zaehle and Friend, 2010). The labile pool is formulated so that around half of the nitrogen required for full leaf-out is taken from retranslocation with a further quarter acquired during the dormant phase, the rest is acquired during the active period.

3.1.3 Canopy nitrogen

JULES includes a process-based scaling-up of leaf level photosynthesis to the the canopy level. There are two options for the canopy scaling up including the 'big-leaf' and a 'multi-layer' approach. In the JULES-CN and JULES-CN$_{layered}$ configurations, to be consistent with JULES-C model, we assume a multi-level canopy with leaf nitrogen decreasing exponentially through the canopy (*CanRadMod 5*). The mean canopy nitrogen content is described by (Mercado et al., 2007):

$$n_{lc} = n_{l0}\exp(-k_n z) \tag{12}$$

where k_n is a constant representing the profile of nitrogen and z represents the fraction of canopy above the layer. Based on observed nitrogen profiles in the Amazon basin (Carswell et al., 2000), a value of 0.78 for k_n was found (Mercado et al., 2007). Equation 12 is independent of leaf area and therefore equates to a constant of proportionality relating PFT-specific top leaf nitrogen (n_{l0}–Table

https://doi.org/10.5194/gmd-2020-205
Preprint. Discussion started: 24 July 2020

1) to the mean canopy nitrogen concentration. Canopy Leaf C:N ratios are resultingly $\tilde{4}4\%$ higher than top leaf ratios.

3.1.4 Allocation

Net Primary Productivity in JULES-C is simply the difference between GPP and autotrophic respiration. In JULES-CN the GPP, NPP_{pot} and autotrophic respiration are calculated at the model timestep (1 hour in JULES-C) prior to any N limitation. These fluxes are then aggregated to the timestep for running TRIFFID (once every 10 days in the JULES-C configuration) so that allocation of carbon can take place. NPP_{pot} supplied to TRIFFID represents the potential amount of carbon that can be allocated to growth and spreading (spreading is the increase in PFT fractional coverage). In order for the NPP to achieve its potential it needs to be able to uptake sufficient inorganic nitrogen. If not enough inorganic nitrogen is available, the system is nitrogen limited and an additional term is required in the carbon balance representing excess carbon which cannot be assimilated into the plant due to lack of available nitrogen (Ψ_c). A positive Ψ_c results in a reduction of carbon use efficiency. The PFT carbon balance is therefore:

$$\frac{dC_v}{dt} = (1-\lambda)\Pi_c - \Lambda_{lc} - \Psi_c \tag{13}$$

where Π_c is the net primary productivity per unit area of PFT (prior to nutrient limitation) and Λ_{lc} is the PFT specific litterfall rate (Section 3.1.5). Any excess carbon (Ψ_c) is considered an additional plant respiration term and at the end of the TRIFFID timestep is used to reduce NPP_{pot} to its actual value. λ is the coefficient for partitioning the NPP between growth and spreading – λ is utilised in increasing the fractional coverage of the vegetation and $(1-\lambda)$ increases the carbon content of the existing vegetated area. λ is a function of the vegetation carbon which itself is a function of the balanced LAI ($\mathcal{L}_b$):

$$\lambda = \begin{cases} 1 & \mathcal{L}_b > \mathcal{L}_{max} \\ \frac{\mathcal{L}_b - \mathcal{L}_{min}}{\mathcal{L}_{max} - \mathcal{L}_{min}} & \mathcal{L}_{min} < \mathcal{L}_b \leq \mathcal{L}_{max} \\ 0 & \mathcal{L}_b \leq \mathcal{L}_{min} \end{cases} \tag{14}$$

Should $\mathcal{L}_b$ fall below $\mathcal{L}_{min}$ then the carbon available for spreading is decreased and $\mathcal{L}_b$ set equal to $\mathcal{L}_{min}$ and the carbon pools re-diagnosed. If $\mathcal{L}_b$ rises above $\mathcal{L}_{max}$ then the carbon available for spreading is increased and $\mathcal{L}_b$ set equal to $\mathcal{L}_{max}$ and the carbon pools re-diagnosed.

The equivalent PFT nitrogen balance is

$$\frac{dN_v}{dt} = (1-\lambda)\Phi - \Lambda_{ln} \tag{15}$$

https://doi.org/10.5194/gmd-2020-205
Preprint. Discussion started: 24 July 2020


Geoscientific Model Development Discussions

where Φ is the plant nitrogen uptake (see below) and Λ_{ln} is the retranslocation of nitrogen from leaves and roots into the plant labile pool (Section 3.1.5 below). The nitrogen available for spreading is a fraction λ of the total available nitrogen and $(1-\lambda)$ is available for growth.

In JULES-CN, on a PFT basis, the nitrogen available for plant uptake is the inorganic soil N pool, N_{in}, split equitably between the PFTs assuming there is no differential ability between PFTs to acquire nitrogen. On a grid cell basis, since the competition for nitrogen depends on the change in carbon over the timestep, larger PFTs have an advantage. The nitrogen uptake in JULES-CN$_{layered}$ is more complicated and is discussed in Section 3.3.1.

The nitrogen available for growth is the total available nitrogen multiplied through by $(1-\lambda)$. Equations 13 and 15 are then solved by bisection such that the nitrogen uptake for growth (Φ_g) is less than or equal to the available nitrogen and the balanced LAI ($\mathcal{L}_b$) remains within the specified upper and lower limits ($\mathcal{L}_{min}$,$\mathcal{L}_{max}$). Following the solution of $\frac{dN_v}{dt}$ the carbon store and balanced LAI ($\mathcal{L}_b$) is updated and the leaf, root and wood pools derived following the allometric equations (Equations 2-4).

The remaining proportion (λ) of NPP and nitrogen after growth is is allocated to spreading. The nitrogen demand for spreading is equal to the carbon allocated to spreading scaled by the whole plant stoichiometry:

$$\Phi_s = \frac{N_v}{C_v}\left(\Pi_c - \frac{dC_v}{dt} - \Psi_s\right) \tag{16}$$

where Ψ_s is the excess carbon term from spreading and $\frac{N_v}{C_v}$ defines the whole plant C:N ratio. The equation is solved such that $(\Phi_s + \Phi_g) \leq N_{avail}$ and Ψ_s is minimised.

Total excess carbon per PFT is therefore the combination of those from growth and spreading

$$\Psi = \Psi_s + \Psi_g \tag{17}$$

Total nitrogen uptake per PFT is therefore the combination of those from growth and spreading

$$\Phi = \Phi_s + \Phi_g \tag{18}$$

The total gridbox nitrogen uptake and excess carbon are therefore the PFT fraction (v_i) weighted total:

$$\Phi = \sum_i v_i \Phi_i \tag{19}$$

$$\Psi = \sum_i v_i \Psi_i \tag{20}$$

https://doi.org/10.5194/gmd-2020-205
Preprint. Discussion started: 24 July 2020


Geoscientific Model Development Discussions
Open Access
EGU

This is the excess carbon (Ψ) that is considered an additional plant respiration term and at the end of the TRIFFID timestep and is used to reduce NPP_{pot} to its actual value.

Carbon and nitrogen allocated to spreading allow the vegetation to expand onto bare ground. Where space is limiting the vegetation competes for space with some carbon being turned over as litter. This is handled in the Lotka-Volterra competition routines (see Clark et al. (2011) for full details). Nitrogen only indirectly affects competition through the PFT specific allometric relationships. The competition code updates the vegetation fractions (v_i).

3.1.5 Litter Production

Litter is produced by the turnover of the leaf, wood and root pools and through the vegetation dynamics due to large-scale disturbance and density-dependent litter production. The PFT specific litter production (Λ_{lc}) is defined as:

$$\Lambda_{lc} = \gamma_l L_c + \gamma_r R_c + \gamma_w W_c \tag{21}$$

where γ_r and γ_w are parameters and γ_l is a temperature dependent turnover rate consistent with the phenological state (Clark et al. (2011). Total litterfall is made-up of the area-weighted sum of the litterfall from each PFT, along with large-scale disturbance rate, and a density dependent component from intra-PFT competition for space.

$$\Lambda_c = \sum_i v_i \left(\Lambda_{lc,i} + \gamma_{vi} C_{vi} + (\Pi_i - \Psi_i) \sum_j c_{ij} v_j \right) \tag{22}$$

where c_{ij} are the competition coefficients describing the effect of PFT i on j, γ_{vi} is a large scale disturbance term and v_i is the vegetation fraction. The effect of nitrogen limitation on the litter carbon flux is captured in the excess carbon term Ψ_i.

The nitrogen equivalent of the PFT specific litter production (Λ_{ln}) allows for retranslocation of nitrogen from leaves and roots into the labile store.

$$\Lambda_{ln} = (1 - \lambda_l)\gamma_l L_n + (1 - \lambda_r)\gamma_r R_n + \gamma_w W_n \tag{23}$$

where λ_l and λ_r are the retranslocation of leaf and root nitrogen coefficients, set at 0.5 and 0.2 (Zaehle and Friend, 2010). Similarly to the total litter carbon, total litter nitrogen is given by:

$$\Lambda_n = \sum_i v_i \left(\Lambda_{ln,i} + \gamma_{vi} N_{vi} + \Phi_i \sum_j c_{ij} v_j \right) \tag{24}$$

https://doi.org/10.5194/gmd-2020-205
Preprint. Discussion started: 24 July 2020


Geoscientific Model Development Discussions
Open Access
EGU

3.2 Soil Biogeochemistry

The soil biogeochemistry in JULES-CN follows the Roth-C soil carbon model (Jenkinson et al., 1990; Jenkinson and Coleman, 1999) used in JULES-C on the TRIFFID timestep, with the addition of a prognostic soil N model. The soil N model simulates immobilisation and mineralisation in the four pools and, if nitrogen is limiting, slows the decomposition rate of litter into soil organic matter (SOM).

The soil carbon model comprises four carbon pools. Plant litter input is split between two carbon pools of decomposable (DPM) and resistant (RPM) plant material, with the fraction that goes to each depending on the overlying vegetation type. Grasses provide a higher fraction of decomposable litter input and trees provide a higher fraction of resistant litter input. The other two carbon pools are microbial biomass (BIO) and long-lived humified (HUM) pools. The DPM and RPM pools can be characterised as representing litter and BIO and HUM as representing soil organic matter. Carbon from decomposition of all four carbon pools is partly released to the atmosphere, and the rest enters the BIO and HUM pools. The carbon pools are updated according to:

$$\frac{dC_{DPM}}{dt} = f_{DPM}\Lambda_c - R_{DPM} \tag{25}$$

$$\frac{dC_{RPM}}{dt} = (1 - f_{DPM})\Lambda_c - R_{RPM} \tag{26}$$

$$\frac{dC_{BIO}}{dt} = 0.46\beta_R R_{tot} - R_{BIO} \tag{27}$$

$$\frac{dC_{HUM}}{dt} = 0.54\beta_R R_{tot} - R_{HUM} \tag{28}$$

where $R_{tot} = R_{DPM} + R_{RPM} + R_{BIO} + R_{HUM}$ is the total respiration in kg C m^{-2} s^{-1}, t is the time in s, the C_i are the carbon pools in kg C m^{-2}, f_{DPM} is the fraction of litter that goes into DPM (dependent on vegetation type), Λ_c is the total litter input in kg C m^{-2} s^{-1} (equation 22) and $(1 - \beta_R)$ is the fraction of soil respiration that is emitted to the atmosphere. β_R depends on soil texture (see Clark et al. (2011) for more details). The nitrogen pools follow a similar structure to the carbon pools:

$$\frac{dN_{DPM}}{dt} = f_{DPM}\Lambda_N - M_{DPM} \tag{29}$$

$$\frac{dN_{RPM}}{dt} = (1 - f_{DPM})\Lambda_N - M_{RPM} \tag{30}$$

https://doi.org/10.5194/gmd-2020-205
Preprint. Discussion started: 24 July 2020


Geoscientific Model Development Discussions

$$\frac{dN_{BIO}}{dt} = 0.46 I_{tot} - M_{BIO} \tag{31}$$

$$\frac{dN_{HUM}}{dt} = 0.54 I_{tot} - M_{HUM} \tag{32}$$

Inputs into the litter pools (DPM, RPM) are from the litter nitrogen flux (Λ_n in kg N m^{-2} s^{-1}, equation 24) and losses are determined by the pool mineralisation of organic nitrogen into inorganic nitrogen (M_i in kg N m^{-2} s^{-1}). Input into the BIO and HUM nitrogen pools comes from the total immobilisation of inorganic nitrogen into organic nitrogen where $I_{tot} = I_{DPM} + I_{RPM} + I_{BIO} + I_{HUM}$ (in kg N m^{-2} s^{-1}). The C to N ratio of the DPM and RPM pools is a function of litter quality and varies temporally and spatially depending on the contributions of the different PFTs within the grid cell. The C to N ratios of the soil organic pools (HUM and BIO) are fixed by a model parameter (CN_{soil}) with a default value of 10. Mineralisation (M_i) and immobilisation (I_i) fluxes take values that maintain this constant C:N ratio for the HUM and BIO pools.

For each soil carbon pool, the potential respiration - i.e. the respiration rate when the nitrogen in the system is not limiting - is given by ($R_{i,pot}$):

$$R_{i,pot} = k_i C_i F_T(T_{soil}) F_s(s) F_v(v) \tag{33}$$

where the k_i are fixed constants in s^{-1} (Clark et al., 2011). The functions of temperature ($F_T(T_{soil})$) and moisture ($F_s(s)$) depend on the temperature (T_{soil}) and moisture content (s) near the surface. The function $F_v(v)$ depends on the vegetation cover fraction (v). The potential mineralisation of organic N when the system is not N limited ($M_{i,pot}$) is related to the potential respiration rates by the C to N ratio of each pool (CN_i):

$$M_{i,pot} = \frac{R_{i,pot}}{CN_i} \tag{34}$$

The potential immobilisation of inorganic nitrogen into the organic nitrogen pools ($I_{i,pot}$) is related to pool potential respiration ($R_{i,pot}$), the respired fraction (β_R) and the C to N ratio of the destination pool in the decomposition chain (CN_i):

$$I_{i,pot} = \beta_R \frac{R_{i,pot}}{CN_{soil}} \tag{35}$$

When nitrogen is limiting, the respiration of the DPM and RPM pools into the soil organic matter pools is additionally limited by the availability of nitrogen:

$$R_{i,pot} = k_i C_i F_T(T_{soil}) F_s(s) F_v(v) F_N(N) \tag{36}$$

https://doi.org/10.5194/gmd-2020-205
Preprint. Discussion started: 24 July 2020


Geoscientific Model Development Discussions

where i is one of RPM or DPM. $F_N(N)$ is the litter decomposition rate modifier and is given by the ratio of the nitrogen available in the soil to the nitrogen required by decomposition. F_N is limited to a range of 0.0 to 1.0. When F_N is equal to 1, the decomposition, mineralisation and immobilisation take place at the potential rate and the system is not nitrogen limited. Where F_N is less than 1, the availability of N limits the decomposition of litter into soil organic matter. F_N is given by:

$$F_N = \frac{(M_{BIO} + M_{HUM} - I_{BIO} - I_{HUM} + N_{avail})}{(D_{DPM} + D_{RPM})} \tag{37}$$

where N_{avail} is the soil available inorganic nitrogen in kg N m^{-2}. D_{DPM} and D_{RPM} are the net demand associated with decomposition of each of the litter pools:

$$D_i = I_{i,pot} - M_{i,pot} \tag{38}$$

where i is one of RPM or DPM. When the net demand is in excess of the available inorganic nitrogen, the system is nitrogen limited and $F_N(N) < 1.0$. This limitation reduces the soil respiration, mineralisation and immobilisation of the two litter pools (RPM and DPM). The other two organic matter pools (BIO and HUM) always respire, are mineralised and immobilised at the potential rate. The C:N ratio of these two pools are therefore variable in time and are represented as prognostic variables.

If the net mineralisation is positive some of the nitrogen is emitted as gas, according to:

$$N_{gas} = f_{gas}(M_{tot} - I_{tot}) \tag{39}$$

where N_{gas} is the gas emission in kg N m^{-2} s^{-1} and f_{gas} is the fraction of the nitrogen flux that is emitted as gas. $M_{tot} = M_{DPM} + M_{RPM} + M_{BIO} + M_{HUM}$ and is the total mineralisation flux in kg N m^{-2} s^{-1}. Following Thomas et al. (2013), it is assumed that 1% of net mineralisation is emitted as gas (f_{gas} is set to 0.01.)

3.2.1 Vertical discretisation

The vertical discretisation of the soil carbon and nitrogen follows Burke et al. (2017). There is a set of four soil carbon and nitrogen pools (DPM, RPM, BIO, HUM) in every soil model layer. Following Burke et al. (2017) the respiration rate is determined for each soil layer depending on the temperature, moisture conditions and nitrogen availability in that layer. An extra reduction of respiration with depth is included to account for factors that are currently missing in the model such as priming effects, anoxia, soil mineral surface and aggregate stabilisation. The potential respiration of each layer is given by:

$$R_{i,pot}(z) = k_i C_i(z) F_T(T_{soil}(z)) F_s(s(z)) F_v(v) \exp(-\tau_{resp} z) \tag{40}$$

https://doi.org/10.5194/gmd-2020-205
Preprint. Discussion started: 24 July 2020

$F_T(T_{soil}(z))$, $F_s(s(z))$ and $C_i(z)$ are now all dependent on depth. $T_{soil}(z)$ and $s(z)$ are the simulated layered soil temperature and soil moisture content and $C_i(z)$ is the simulated soil carbon content for each layer and pool i. The additional reduction of respiration with depth is exponential, with τ_{resp} an empirical parameter (in m^{-1}) that controls the magnitude of the reduction. The larger the value of τ_{resp}, the more inhibited the respiration is with increasing depth. When nitrogen is limiting, the respiration of the DPM and RPM pools are reduced by a factor of $F_N(N(z))$ which is also now a function of depth and dependent on the available nitrogen in the relevant layer. M_i and I_i are also calculated as a function of depth based on their relationship with respiration.

The vertical mixing of each soil nitrogen pool follows that of the soil carbon pools:

$$\frac{\partial N_{DPM}(z)}{\partial t} = \frac{\partial}{\partial z}\left(D(z)\frac{\partial CN_{DPM}(z)}{\partial z}\right) + f_{dpm}\Lambda_n(z) - M_{DPM}(z) \tag{41}$$

$$\frac{\partial N_{RPM}(z)}{\partial t} = \frac{\partial}{\partial z}\left(D(z)\frac{\partial CN_{RPM}(z)}{\partial z}\right) + (1 - f_{dpm})\Lambda_n(z) - M_{RPM}(z) \tag{42}$$

$$\frac{\partial N_{BIO}(z)}{\partial t} = \frac{\partial}{\partial z}\left(D(z)\frac{\partial CN_{BIO}(z)}{\partial z}\right) + 0.46I_{tot}(z) - M_{BIO}(z) \tag{43}$$

$$\frac{\partial N_{HUM}(z)}{\partial t} = \frac{\partial}{\partial z}\left(D(z)\frac{\partial CN_{HUM}(z)}{\partial z}\right) + 0.54I_{tot}(z) - M_{HUM}(z) \tag{44}$$

I_{tot} is the total immobilisation in kg N m^{-2} s^{-1} in each layer. $D(z)$ is the diffusivity in m^2 s^{-1} and varies both spatially and with depth (Burke et al., 2017). The litter inputs are distributed so that they decline exponentially with depth, with an e-folding depth of 0.2 m. Mineralised gas emissions are calculated for each soil layer, based on the balance of mineralisation and immobilisation in that layer (i.e. Equation 39 is repeated for every layer).

3.3 Inorganic Nitrogen

The inorganic nitrogen pool is the sum of deposition, fixation, immobilisation losses, mineralisation inputs, gridbox mean plant uptake and inorganic N losses through leaching and gaseous emission. For the non-layered case (JULES-CN), these terms are simply added together:

$$\frac{dN_{in}}{dt} = N_{dep} + \sum_i v_i F_i - \sum_i v_i \Phi_i + M_{net} - N_{leach} - N_{turnover} \tag{45}$$

where N_{in} is the inorganic nitrogen in kg N m^{-2}. N_{dep} is prescribed nitrogen deposition in kg N m^{-2} s^{-1}. The plant fixation (F_i) and uptake (Φ_i) are described in Sections 3.1.1 and 3.1.4. (M_{net}) is the net mineralisation which is the difference between M_{tot} and I_{tot} reduced by N_{gas}. (Section 3.2).

https://doi.org/10.5194/gmd-2020-205
Preprint. Discussion started: 24 July 2020


Geoscientific Model Development Discussions
Open Access
EGU

The loss of nitrogen from the inorganic pool is a function of leaching (N_{leach}) and an additional turnover ($N_{turnover}$).

$$N_{turnover} = \gamma_n N_{in} \tag{46}$$

where γ_n is a tunable parameter. This additional term represents missing processes relating to the gaseous loss of inorganic nitrogen and limits the effective mineral N pool size. Without this additional turnover available N may increase excessively, potentially due to excessive biological fixation in regions that are generally unlimited. In the current model configuration this parameter is set to 1.0 (360 $day^{-}1$) such that the whole pool turns over once every model year. This results in an effective saturation limit of 0.002 KgN m-2 consistent with Parton et al. (1993).

The leaching of nitrogen through the profile is assumed to be a function of the net flux of moisture through the soil profile, the concentration of inorganic N, and a parameter (β) representing the effective solubility of nitrogen. β has a value of 0.1. based on the sorption buffer coefficient of Ammonia (Gerber et al., 2010) although here it represents the sorption of all inorganic nitrogen species.

$$N_{leach} = \beta(N_{in}/\theta_{1\mathrm{m}})Q_{subsurface} \tag{47}$$

where $\theta_{1\mathrm{m}}$ is the soil water content in the top 1m of soil in kg m^{-2} (so the inorganic nitrogen is assumed to occupy the top 1m of soil), and $Q_{subsurface}$ is the total subsurface runoff in kg m^{-2} s^{-1}.

3.3.1 Vertical discretisation of inorganic nitrogen

In JULES-CN$_{layered}$, there is an inorganic nitrogen pool in each soil layer. The dynamics are very similar to Equation 45, but every component now varies with depth, so:

$$\frac{dN_{in}(z)}{dt} = N_{dep}(z) + \sum_i v_i F_i f_{1,i}(z) - \sum_i v_i \Phi_i f_{2,i}(z) + M_{net}(z) - N_{flux}(z) - N_{turnover}(z) \tag{48}$$

The net mineralisation flux ($M_{net}(z)$) is the difference between $M_{tot}(z)$ and $I_{tot}(z)$ reduced by $\mathrm{N}_{gas}(z)$ from each layer (see Section 3.2.1). Nitrogen deposition ($N_{dep}(z)$) is added to the uppermost soil layer. Inputs from plant nitrogen fixation from PFT i are distributed according to the root profile of the plants, i.e.

$$f_{1,i}(z) = \frac{f_{root,i}(z)}{\int_0^{z_{max}} f_{root,i}(z)dz} \tag{49}$$

where $f_{root}(z)$ is the volumetric root fraction at a given depth.

Turnover ($N_{turnover}(z)$) occurs in each layer, but with an exponential decay with depth as for the soil decomposition, which empirically represents the factors that reduce the soil activity with depth.

https://doi.org/10.5194/gmd-2020-205
Preprint. Discussion started: 24 July 2020


Geoscientific Model Development Discussions

The turnover term thus becomes:

$$N_{turnover}(z) = \gamma_n N_{in}(z) \exp(-\tau_{resp} z) \tag{50}$$

This leaves two terms in Equation 48: the plant uptake term ($\sum_i v_i \Phi_i f_{2,i}(z)$) and the N_{flux} term, which replaces the leaching term from Equation 45. These have a more process-based representation in the layered case. Plants cannot access all the inorganic nitrogen. Firstly, we assume that if a soil layer is frozen then plants cannot uptake any of the nitrogen in that layer. Secondly, we assume that they only have direct access to a certain fraction of the soil, according to their root fraction, $f_{root,i}$ (which reduces with depth). So for each PFT, i, there is an 'available' inorganic nitrogen pool, which at equilibrium is as follows:

$$N_{avail,i} = f_{root,i} N_{in} \tag{51}$$

As nitrogen is taken up from the available pool around the roots, there will be a delay in the area around the roots getting 're-filled'. We assume that it is constantly diffusing back to the equilibrium state where the concentration is constant both horizontally and vertically within each layer, and thus after the extraction on a particular TRIFFID timestep we update the available N pool according to:

$$\frac{N_{avail,i}}{dt} = \gamma_{diff}(f_{root,i} N_{in} - N_{avail,i}) \tag{52}$$

where γ_{diff} is the rate of diffusion back to the equilibrium, set by default to 100 [360 day]$^{-1}$. Any fixation goes directly into the available pool, and other fluxes are simply added according to the ratio of the available to total inorganic N pools at equilibrium (thus the available pool would always follow Equation51 were it not for the fixation and uptake by plants). Plant uptake is extracted entirely from the available N pool, and the dependence on depth is according to the same profile as the available N, i.e.

$$f_{2,i}(z) = \frac{N_{avail,i}(z)}{\int_0^{z_{max}} N_{avail,i}(z) dz} \tag{53}$$

Leaching is now done in a process-based manner, where the inorganic N is transported through the soil profile by the soil water fluxes. Thus in Equation 48 we have the following term:

$$N_{flux}(z) = \beta dz_n \frac{d}{dz}\left(W_{flux} \frac{N_{in}(z)}{\theta}\right) \tag{54}$$

where θ is the soil water content in kg m^{-2} and W_{flux} is the flow rate of the water through the soil in kg m^{-2} s^{-1}. Multiplying by dz_n gives the change in N content for each layer, n. The total leaching is then the sum of all nitrogen that leaves the soil by lateral runoff or out of the bottom soil layer.

4 Historical simulations

Global transient simulations were carried out following the protocol for the S2 experiments in TRENDY (Sitch et al., 2015). Forcing consisted of time-varying CO_2, and climate from the CRU-NCEP data-set (v4, 1901-2012, Viovy N. 2011 CRU-NCEPv4. CRUNCEP dataset). The fraction of

https://doi.org/10.5194/gmd-2020-205
Preprint. Discussion started: 24 July 2020


Geoscientific Model Development Discussions
Open Access
EGU

agriculture in each grid cell (Hurtt et al., 2011) was set to the pre-industrial value. Nitrogen deposition was time-varying and was taken from a ACCMIP multi-model data set interpolated to annual fields (Lamarque et al., 2013). The model resolution was N96 (1.875° longitude x 1.25° latitude).

Results from three different JULES model configurations are presented here:

- JULES-C represents the soil and vegetation carbon cycle in a manner comparable with HadGEM2-ES (Jones et al., 2011).
- JULES-CN is the nitrogen enabled version of JULES-C.
- JULES-CN$_{layered}$ is a version of JULES-CN with vertically discretised soil biochemistry.

In each case five PFTs were used: broadleaf trees, needleleaf trees (NET), C3 and C4 grass and shrubs. Plant competition was allowed, with TRIFFID updating vegetation fractions on a 10 day time step. The sole difference between JULES-C and JULES-CN is the inclusion of the nitrogen cycle. JULES-CN$_{layered}$ additionally has vertically discretised soil biogeochemistry. There are no differences in any of the shared model parameters.

The simulations were initialised using pre-industrial conditions. They were spun up by repeating the time period 1860-1870 until the change was less than 0.01 % decade^{-1} globally. The soil carbon distribution in JULES-CN$_{layered}$ is particularly slow to reach equilibrium. Therefore the 'modified accelerated decomposition' technique (modified-AD) described by Koven et al. (2013) was used to spin the soil carbon in these versions up to an initial pre-industrial equilibrium distribution (Burke et al., 2017). Further spin up was then carried out for these layered models using repeated pre-industrial conditions until the change in soil carbon was less than 0.01 % decade^{-1} globally. It should be noted that neither transient land-use change or fertiliser were included in any of these simulations.

5 Results

This paper focuses on the differences between selected model configurations introduced by including the explicit nitrogen cycle within JULES. When available, we additionally use any observational based estimates to evaluate the quality of the simulations. First a broad-brush comparison between JULES-CN, JULES-C and JULES-CN$_{layered}$ is made. This is followed by a more complete discussion comparing JULES-CN with JULES-C. Finally the extra processes supplied by JULES-CN$_{layered}$ are assessed. For completeness figures often include both JULES-CN and JULES-CN$_{layered}$ but JULES-CN$_{layered}$ is only discussed at the end of the results.

https://doi.org/10.5194/gmd-2020-205
Preprint. Discussion started: 24 July 2020


Geoscientific Model Development Discussions

5.1 Summary of carbon and nitrogen stocks and fluxes

Figure 4 provides an overview of the stocks and fluxes of carbon and nitrogen in JULES-CN and JULES-CN$_{layered}$ and compares them with JULES-C. As expected for a present-day simulation, the majority of stocks and fluxes are very similar for JULES-C and JULES-CN. The main difference is the present-day NPP which is ~12% higher in JULES-C than in JULES-CN. This is a direct consequence of nitrogen limitation which restricts the ability of the plants to utilise all of the carbon. There is also a small reduction in the GPP of ~4% caused by small differences in the vegetation distribution and indirectly resulting from the nitrogen limitation.

Soil organic nitrogen and vegetation nitrogen are both consistent with the available observation-based estimates of stocks as are the nitrogen fixation, nitrogen losses and nitrogen deposition. Fixation is tuned to be approximately 100 TgN year^{-1} in the present day. The majority of N losses occur via the gaseous pathway with total losses of 135 TgN/yr^{-1} for JULES-CN. Leaching is fairly low at 7 TgN/yr^{-1} for JULES-CN compared to estimates of leaching, which are as high as 25 - 55% of N inputs in European forests (Dise et al., 2009) and range between 59 and 118 TgN/yr^{-1} in the available observations (Boyer et al., 2006; Galloway et al., 2004; Gruber and Galloway, 2008). Nitrogen uptake and net mineralisation are relatively high and are fairly similar in magnitude implying a largely closed cycling of nutrients between vegetation and soil. However, there is no nitrogen fertiliser applied to the soil in the model meaning nitrogen inputs are expected to be lower than in reality. These nitrogen stocks and fluxes are also consistent with results from other models such as: Xu-Ri and Prentice (2008), Smith et al. (2014), Zaehle (2013b) and von Bloh et al. (2018).

5.2 Impact of nitrogen limitation on net primary productivity

Figure 5 shows the biome-based response ratio of net primary productivity. The response ratio is defined as the ratio of the NPP when nitrogen is unlimited (NPP_{pot}) compared with the nitrogen limited NPP. Both of these diagnostics are output from the JULES simulations. All biomes have a response ratio of greater than 1 in both the model and observations which means that adding extra nitrogen to the system will enhance the achieved NPP. Globally the response ratio falls within the observed error bars and for the majority of the biomes including the tropical forests and the tundra the model response ratios fall within the range of uncertainties of the observations. However, LeBauer and Treseder (2008) suggests tropical savannah is not very nitrogen limited, whereas in JULES-CN tropical savannah is a highly limited biome. Further work is required to understand why tropical savannah is so limited. Figure 6 shows the spatial distribution of the model simulated response ratio. Green areas are not very nitrogen limited and yellow areas are more nitrogen limited. There are distinct regions of nitrogen limitation - northern Australia, the Sahel, western Europe and

https://doi.org/10.5194/gmd-2020-205
Preprint. Discussion started: 24 July 2020

parts of Siberia. Much of the global land surface has relatively weak nitrogen limitation.

In the model the soil carbon decomposition can be limited when the nitrogen available in the soil is less than the nitrogen required by decomposition. This process does not play a major role in our simulations.

5.2.1 Ecosystem residence times

The zonal total soil and vegetation carbon stocks are shown in Figure 7. The vegetation carbon is very similar for both JULES-C and JULES-CN as expected from Figure 4 and is consistent with the available observations. There are some differences in the soil carbon in the northern high latitudes with JULES-CN having slightly less soil carbon than JULES-C. This is a consequence of the higher nitrogen limitation on JULES-CN leading to less litter fall and subsequently less soil carbon. The ecosystem residence time is defined as the total ecosystem carbon divided by the GPP. This is shown in Figure 8 for the biomes introduced in Figure 5. These residence times have been estimated annually on a grid cell by grid cell basis and then aggregated to a multi-annual mean per biome. The observational values were derived in a similar way using spatial data from Carvalhais et al. (2014). In general the residence times are fairly similar for JULES-C and JULES-CN except for the tundra biome where the residence time for JULES-CN is much longer than that for JULES-C. This is an over estimation of the residence time for this biome, however, JULES-CN is missing some key permafrost processes which will lead to an improvement (see Section 3.2.1).

The soil organic nitrogen (Figure 9) shows a similar distribution to the soil carbon (Figure 7) reflecting the relatively consistent C to N ratio of the soil within the model. The observed soil organic nitrogen content is slightly higher at all latitudes than simulated by JULES-CN particularly in the northern tundra region.

5.2.2 Carbon-use efficiency

Carbon use efficiency (CUE) is defined as the ratio of net carbon gain to gross carbon assimilation during a given period (NPP/GPP). This represents the capacity of the plants to allocate carbon from photosynthesis to the terrestrial biomass. In the model nitrogen limitation restricts the ability of plants to allocate carbon and reduces the carbon use efficiency. Figure 10 shows the zonal total GPP and NPP for JULES-CN and JULES-C. As expected from Figure 4 the NPP and GPP have very similar latitudinal profiles for the two model configurations. Both JULES-C and JULES-CN have a higher GPP in the tropics that the observations but they are more comparable in the extra-tropical latitudes where the GPP tends to be smaller. The NPP in JULES-CN is less than JULES-C and generally closer to the MODIS observations particularly in the tropics. Figure 10 also shows the zonal

https://doi.org/10.5194/gmd-2020-205
Preprint. Discussion started: 24 July 2020

mean CUE. JULES-CN has a lower CUE than JULES-C for all latitudes. On average it is 0.44 for JULES-CN and 0.49 for JULES-C. JULES-CN has a consistently high bias of ∼0.09 compared to the Kim et al. (2018) observation-based data set. This bias is relatively constant with latitude. Figure 11 shows the changes in these carbon fluxes for the period 1860-2007 with respect to the multi-annual mean period of 1860-1899. Changes over time are shown to enable the differences between the two different model configurations to be more easily compared. Apparently small differences between JULES-C and JULES-CN in the NPP and GPP become more noticeable in the CUE. The small differences between JULES-C and JULES-CN in GPP are caused by structural changes in the vegetation in particular small changes in the vegetation distribution and a slight increase in bare soil in JULES-CN. In the case of NPP - JULES-C increases quicker than JULES-CN because JULES-CN becomes progressively more nitrogen limited. The change in CUE shows the impact of the nitrogen cycle on the uptake of carbon by the vegetation in JULES-CN over the twentieth century. There is an increase in CUE in both configurations, mainly caused by CO_2 fertilisation, but this is limited by nitrogen in the JULES-CN configuration.

5.2.3 Net ecosystem exchange

A key measure of a land carbon cycle model is how well it simulates the temporal variation of the land carbon sink, which is the difference between Net Ecosystem Exchange (NEE) and the flux of carbon to the atmosphere from land-use change. The interannual variability in the sink is dominated by the variability of NEE, which is itself correlated with the magnitude of the temperature-carbon cycle feedback in the tropics (Cox et al., 2013). As a result, simulation of NEE variability is highly relevant to climate-carbon cycle projections (Wenzel et al., 2016).

Figure 12 compares global annual mean values of Net ecosystem exchange (NEE; defined as NPP - heterotrophic respiration) for JULES-C and JULES-CN to observation-based estimates from the Global Carbon Project. We specifically focus on the years from 1960 to 2009, which is the maximum overlap period between the model simulations and the GCP annual budget data (Friedlingstein et al., 2019). To avoid the circularity of using GCP estimates of NEE which are themselves derived from land-surface models, we instead calculate the GCP estimates of NEE as the residual of the best estimates of the total emissions from fossil fuel (FF) plus land-use change (LU), and the rate of increase of the carbon content of the atmosphere (F_a) plus the ocean (F_o):

$$NEE_{gcp} = FF + LU - F_a - F_o \tag{55}$$

The observations and both of the models show an upward trend in NEE but with very significant interannual variability (Figure 12). Due to nitrogen limitations on CO_2 fertilization, mean NEE in JULES-CN (1.66 Pg C/yr) is lower than in JULES-C (2.06 Pg C/yr), and also lower than the

https://doi.org/10.5194/gmd-2020-205
Preprint. Discussion started: 24 July 2020

Geoscientific Model Development Discussions
Open Access
EGU

	Mean (Pg C/yr)	Trend (Pg C/yr/yr)	IAV (Pg C/yr)	r
JULES-C	2.06	0.034	1.31	0.63
JULES-CN	1.66	0.025	0.86	0.71
GCP(residual)	2.11	0.027	1.01	

Table 2. Statistics of NEE from JULES-C, JULES-CN, and the GCP observation-based estimates (Friedlingstein et al. 2019), over the period from 1960 to 2009 inclusive. Columns 2-4 show respectively the mean, linear trend, and the interannual variability (standard deviation) around that trend. Column 5 shows the correlation coefficient between each model NEE timeseries and the GCP timeseries.

estimate from GCP (2.11 Pg C/yr). However, JULES-CN outperforms JULES-C on all of the other key metrics of the NEE variation. JULES-CN produces a smaller but much more realistic trend in NEE, and a smaller and more realistic interannual variability about that trend (see Table 5.2.3). The correlation coefficient for NEE between the JULES-CN and GCP estimates (r=0.71) is also improved compared to JULES-C (r=0.63). There remains a significant underestimate of NEE in the years following the Pinatubo volcanic eruption, most likely due to the neglect of diffuse-radiation fertilization in these versions of JULES (Mercado et al., 2009). However, it is especially notable that JULES-CN significantly reduces the systematic overestimate of NEE seen in JULES-C during extended La Nina periods, such as the years centred around 1974 and 2000 (Figure 12).

5.3 Impact of vertical discretisation of soil biochemistry

Over the tropics and southern latitudes, JULES-CN$_{layered}$ is very comparable to JULES-CN. The main differences occur in the northern regions where there is soil freezing – adding vertically discretised soil biogeochemistry to JULES-CN has the most impact in the northern high latitudes. The soil in JULES-CN$_{layered}$ has more inorganic nitrogen (Figure 4) but it is not all accessible for the plants to uptake because the nitrogen uptake is limited by frozen soil. This means that in regions with frozen soil JULES-CN$_{layered}$ is slightly more nitrogen limited than JULES-CN (Figure 5). Globally JULES-CN$_{layered}$ is possible also slightly more limited than the observations suggest (Figure 5). The biggest difference between JULES-CN$_{layered}$ and JULES-CN is for the boreal and coniferous biome where the response ratio (potential NPP/ achieved NPP) for JULES-CN is 1.32 of that of JULES-CN$_{layered}$ is 1.48.

This additional limitation of nitrogen uptake caused by frozen soils means that JULES-CN$_{layered}$ has less total vegetation. However it also has more soil organic carbon and soil organic nitrogen (Figure 9) because the colder soil temperatures deeper in the soil profile inhibits soil carbon decomposition. This improves the estimate of the residence tome of carbon in the tundra (Figure 8). The extra inorganic nitrogen in JULES-CN$_{layered}$ (Figure 9) is mainly stored deeper in the soil profile and some of it within the permafrost itself. The vertical discretisation of the soil organic carbon and

https://doi.org/10.5194/gmd-2020-205
Preprint. Discussion started: 24 July 2020

nitrogen results in a longer soil residence time in JULES-CN$_{layered}$ (defined as soil organic carbon / soil respiration). This improved representation of the soil biogeochemistry will have implications for simulations of climate change in the northern high latitudes.

6 Conclusions

In this paper we have documented a model to quantify the impact of coupling the nitrogen cycle with the carbon cycle in a fully dynamic vegetation model. In this model, nitrogen limitation affects NPP and how the carbon is allocated but it only indirectly affects the photosynthesis via leaf area development. This enables the carbon use efficiency (ratio of net carbon gain to gross carbon assimilation) to respond to changing nitrogen availability. Since the CUE affects the ability of the land surface to uptake carbon in a changing climate, this will impact carbon budgets under future projections of climate change. This scheme (based on JULES-CN) has been included within UKESM1 (Sellar et al., 2019).

Overall the nitrogen enabled configuration of JULES – JULES-CN – produces a more realistic trend in the net ecosystem exchange (NEE) and the interannual variability of NEE about that trend. It also produces an improved estimate of NPP in the northern high latitudes. For other regions and diagnostics the simulation of present-day state and behaviour is not substantially different between JULES-C and the nitrogen-enabled configuration, JULES-C. This is largely because JULES-C has been tuned to replicate observed carbon stores and fluxes and therefore implicitly includes a level of nitrogen availability. What JULES-C lacks is a mechanism for this to change substantially in time – either under more limiting conditions as elevated CO_2 outpaces demand for nutrients (e.g.Zaehle (2013b)), or under conditions of increased nitrogen availability due to anthropogenic deposition or climate-induced mineralisation (Meyerholt et al., 2020b; Zaehle and Dalmonech, 2011). The response of the nitrogen cycle in JULES under changes in climate and CO_2 conditions–which will be affected by nutrient limitations–will be quantified and assessed in subsequent work.

An extended version of the nitrogen-enabled model model additionally includes the vertical discretisation of the soil biogeochemistry model. This configuration improves the ecosystem residence times in the tundra. This more detailed representation of permafrost biogeochemistry in the northern high latitudes will used to understand the impact of the coupled carbon and nitrogen cycle on the permafrost carbon feedback.

https://doi.org/10.5194/gmd-2020-205
Preprint. Discussion started: 24 July 2020


Geoscientific Model Development Discussions

Code Availability

The JULES code used in these simulations is available from the Met Office Science Repository Service (registration required) at https://code.metoffice.gov.uk/trac/jules. To access the code a freely available non-commercial research licence is required (https://jules-lsm.github.io/). The suites required for running JULES are available here: https://code.metoffice.gov.uk/trac/roses-u. JULES-CN is u-ah896, JULES-C is u-ah932 and JULES-CN$_{layered}$ is u-ai571.

Competing Interests

The authors declare that they have no conflict of interest.

Author contributions. Andy Wiltshire designed the model in collaboration with the rest of the co-authors and wrote the first draft of the text. Eleanor Burke and Sarah Chadburn added the layered soil biogeochemistry. Peter Cox performed the analysis of inter-annual variability. All authors reviewed the paper and proposed improvements.

Acknowledgements. This work has received funding from the European Union's Horizon 2020 research and innovation programme under grant agreement No 641816 Coordinated Research in Earth Systems and Climate: Experiments, kNowledge, Dissemination and Outreach (CRESCENDO). Andy Wiltshire and Eleanor Burke were also supported by the Joint UK BEIS/Defra Met Office Hadley Centre Climate Programme (GA01101). Sarah Chadburn was supported by the Natural Environment Research Council (grant no. NE/M01990X/1 and NE/R015791/1). Peter Cox was supported by the European Research Council (ERC) ECCLES project, grant agreement number 742472. Sönke Zaehle was also supported by the European Research Council (ERC) under the European Union's Horizon 2020 research and innovation programme (grant agreement No 647204).

https://doi.org/10.5194/gmd-2020-205
Preprint. Discussion started: 24 July 2020

References

Arora, V. K., Katavouta, A., Williams, R. G., Jones, C. D., Brovkin, V., Friedlingstein, P., Schwinger, J., Bopp, L., Boucher, O., Cadule, P., et al.: Carbon-concentration and carbon-climate feedbacks in CMIP6 models, and their comparison to CMIP5 models, Biogeosciences Discussions, pp. 1–124, 2019.

Avitabile, V., Herold, M., Heuvelink, G. B., Lewis, S. L., Phillips, O. L., Asner, G. P., Armston, J., Ashton, P. S., Banin, L., Bayol, N., et al.: An integrated pan-tropical biomass map using multiple reference datasets, Global change biology, 22, 1406–1420, 2016.

Ballantyne, A., Smith, W., Anderegg, W., Kauppi, P., Sarmiento, J., Tans, P., Shevliakova, E., Pan, Y., Poulter, B., Anav, A., et al.: Accelerating net terrestrial carbon uptake during the warming hiatus due to reduced respiration, Nature Climate Change, 7, 148, 2017.

Batjes, N.: Total carbon and nitrogen in the soils of the world, European Journal of Soil Science, 65, 10–21, 2014.

Batjes, N. H.: Harmonized soil property values for broad-scale modelling (WISE30sec) with estimates of global soil carbon stocks, Geoderma, 269, 61–68, 2016.

Best, M. J., Pryor, M., Clark, D. B., Rooney, G. G., Essery, R. L. H., Ménard, C. B., Edwards, J. M., Hendry, M. A., Porson, A., Gedney, N., Mercado, L. M., Sitch, S., Blyth, E., Boucher, O., Cox, P. M., Grimmond, C. S. B., and Harding, R. J.: The Joint UK Land Environment Simulator (JULES), model description â€“ Part 1: Energy and water fluxes, Geoscientific Model Development, 4, 677–699, doi:10.5194/gmd-4-677-2011, http://www.geosci-model-dev.net/4/677/2011/, 2011.

Boyer, E. W., Howarth, R. W., Galloway, J. N., Dentener, F. J., Green, P. A., and Vörösmarty, C. J.: Riverine nitrogen export from the continents to the coasts, Global Biogeochemical Cycles, 20, 2006.

Burke, E. J., Chadburn, S. E., and Ekici, A.: A vertical representation of soil carbon in the JULES land surface scheme (vn4.3_permafrost) with a focus on permafrost regions, Geoscientific Model Development, 10, 959–975, doi:10.5194/gmd-10-959-2017, http://www.geosci-model-dev.net/10/959/2017/, 2017.

Carswell, F., Meir, P., Wandelli, E., Bonates, L., Kruijt, B., Barbosa, E., Nobre, A., Grace, J., and Jarvis, P.: Photosynthetic capacity in a central Amazonian rain forest, Tree Physiology, 20, 179–186, 2000.

Carvalhais, N., Forkel, M., Khomik, M., Bellarby, J., Jung, M., Migliavacca, M., Mu, M., Saatchi, S., Santoro, M., Thurner, M., et al.: Global covariation of carbon turnover times with climate in terrestrial ecosystems, Nature, 514, 213–217, 2014.

Chadburn, S., Burke, E., Essery, R., Boike, J., Langer, M., Heikenfeld, M., Cox, P., and Friedlingstein, P.: An improved representation of physical permafrost dynamics in the JULES land-surface model, Geoscientific Model Development, 8, 1493–1508, doi:10.5194/gmd-8-1493-2015, http://www.geosci-model-dev.net/8/1493/2015/, 2015.

Clark, D. B., Mercado, L. M., Sitch, S., Jones, C. D., Gedney, N., Best, M. J., Pryor, M., Rooney, G. G., Essery, R. L. H., Blyth, E., Boucher, O., Harding, R. J., Huntingford, C., and Cox, P. M.: The Joint UK Land Environment Simulator (JULES), model description Part 2: Carbon fluxes and vegetation dynamics, Geoscientific Model Development, 4, 701–722, doi:10.5194/gmd-4-701-2011, http://www.geosci-model-dev.net/4/701/2011/, 2011.

https://doi.org/10.5194/gmd-2020-205
Preprint. Discussion started: 24 July 2020

Cleveland, C. C., Townsend, A. R., Schimel, D. S., Fisher, H., Howarth, R. W., Hedin, L. O., Perakis, S. S., Latty, E. F., Von Fischer, J. C., Elseroad, A., et al.: Global patterns of terrestrial biological nitrogen (N2) fixation in natural ecosystems, Global biogeochemical cycles, 13, 623–645, 1999.

Collalti, A. and Prentice, I.: Is NPP proportional to GPP? Waring's hypothesis 20 years on, Tree physiology, 39, 1473–1483, 2019.

Collins, W., Bellouin, N., Doutriaux-Boucher, M., Gedney, N., Halloran, P., Hinton, T., Hughes, J., Jones, C., Joshi, M., Liddicoat, S., et al.: Development and evaluation of an Earth-System model–HadGEM2, Geoscientific Model Development, 4, 1051–1075, 2011.

Cox, P. M.: Description of the TRIFFID dynamic global vegetation model, Tech. rep., Met Office Hadley Centre, Exeter, UK, http://www.metoffice.gov.uk/media/pdf/9/h/HCTN_24.pdf, 2001.

Cox, P. M., Pearson, D., Booth, B. B., Friedlingstein, P., Huntingford, C., Jones, C. D., and Luke, C. M.: Sensitivity of tropical carbon to climate change constrained by carbon dioxide variability, Nature, 494, 341–344, 2013.

Davies-Barnard, T. and Friedlingstein, P.: The Global Distribution of Biological Nitrogen Fixation in Terrestrial Natural Ecosystems, Global Biogeochemical Cycles, 34, e2019GB006 387, doi:10.1029/2019GB006387, https://agupubs.onlinelibrary.wiley.com/doi/abs/10.1029/2019GB006387, e2019GB006387 2019GB006387, 2020.

Davies-Barnard, T., Meyerholt, J., Zaehle, S., Friedlingstein, P., Brovkin, V., Fan, Y., Fisher, R. A., Jones, C. D., Lee, H., Peano, D., Smith, B., Wårlind, D., and Wiltshire, A.: Nitrogen Cycling in CMIP6 Land Surface Models: Progress and Limitations, Biogeosciences Discussions, 2020, 1–32, doi:10.5194/bg-2019-513, https://www.biogeosciences-discuss.net/bg-2019-513/, 2020.

Dise, N. B., Rothwell, J. J., Gauci, V., van der Salm, C., and de Vries, W.: Predicting dissolved inorganic nitrogen leaching in European forests using two independent databases, Science of The Total Environment, 407, 1798–1808, doi:10.1016/j.scitotenv.2008.11.003, http://www.sciencedirect.com/science/article/pii/S0048969708011261, 2009.

Friedlingstein, P., Jones, M., O'Sullivan, M., Andrew, R., Hauck, J., Peters, G., Peters, W., Pongratz, J., Sitch, S., Le Quéré, C., et al.: Global carbon budget 2019, Earth System Science Data, 11, 1783–1838, 2019.

Galloway, J. N., Dentener, F. J., Capone, D. G., Boyer, E. W., Howarth, R. W., Seitzinger, S. P., Asner, G. P., Cleveland, C. C., Green, P., Holland, E. A., et al.: Nitrogen cycles: past, present, and future, Biogeochemistry, 70, 153–226, 2004.

Gerber, S., Hedin, L. O., Oppenheimer, M., Pacala, S. W., and Shevliakova, E.: Nitrogen cycling and feedbacks in a global dynamic land model, Global Biogeochemical Cycles, 24, 2010.

Group, G. S. D. T.: Global Gridded Surfaces of Selected Soil Characteristics (IGBP-DIS).[Global Gridded Surfaces of Selected Soil Characteristics (International Geosphere-Biosphere Programme-Data and Information System)]., 2000.

Gruber, N. and Galloway, J. N.: An Earth-system perspective of the global nitrogen cycle, Nature, 451, 293, 2008.

Harper, A. B., Wiltshire, A. J., Cox, P. M., Friedlingstein, P., Jones, C. D., Mercado, L. M., Sitch, S., Williams, K., and Duran-Rojas, C.: Vegetation distribution and terrestrial carbon cycle in a carbon-cycle configura-

https://doi.org/10.5194/gmd-2020-205
Preprint. Discussion started: 24 July 2020

tion of JULES4. 6 with new plant functional types, Geosci. Model Dev. Discuss., https://doi.org/10.5194/gmd-2017-311, 2018.

Hashimoto, S., Carvalhais, N., Ito, A., Migliavacca, M., Nishina, K., and Reichstein, M.: Global spatiotemporal distribution of soil respiration modeled using a global database, Biogeosciences, 12, 4121–4132, 2015.

Houlton, B. Z., Wang, Y.-P., Vitousek, P. M., and Field, C. B.: A unifying framework for dinitrogen fixation in the terrestrial biosphere, Nature, 454, 327–330, 2008.

Hurtt, G. C., Chini, L. P., Frolking, S., Betts, R., Feddema, J., Fischer, G., Fisk, J., Hibbard, K., Houghton, R., Janetos, A., et al.: Harmonization of land-use scenarios for the period 1500–2100: 600 years of global gridded annual land-use transitions, wood harvest, and resulting secondary lands, Climatic change, 109, 117–161, 2011.

Jenkinson, D. and Coleman, K.: A model for the turnover of carbon in soil—Model description and windows user guide, Rothamsted Research, Harpenden, UK, 1999.

Jenkinson, D. S., Andrew, S. P. S., Lynch, J. M., Goss, M. J., and Tinker, P. B.: The Turnover of Organic Carbon and Nitrogen in Soil [and Discussion], Philosophical Transactions: Biological Sciences, 329, 361–368, http://www.jstor.org/stable/76840, 1990.

Jones, C. D., Hughes, J. K., Bellouin, N., Hardiman, S. C., Jones, G. S., Knight, J., Liddicoat, S., O'Connor, F. M., Andres, R. J., Bell, C., Boo, K.-O., Bozzo, A., Butchart, N., Cadule, P., Corbin, K. D., Doutriaux-Boucher, M., Friedlingstein, P., Gornall, J., Gray, L., Halloran, P. R., Hurtt, G., Ingram, W. J., Lamarque, J.-F., Law, R. M., Meinshausen, M., Osprey, S., Palin, E. J., Parsons Chini, L., Raddatz, T., Sanderson, M. G., Sellar, A. A., Schurer, A., Valdes, P., Wood, N., Woodward, S., Yoshioka, M., and Zerroukat, M.: The HadGEM2-ES implementation of CMIP5 centennial simulations, Geoscientific Model Development, 4, 543–570, doi:10.5194/gmd-4-543-2011, https://www.geosci-model-dev.net/4/543/2011/, 2011.

Jung, M., Reichstein, M., Margolis, H. A., Cescatti, A., Richardson, A. D., Arain, M. A., Arneth, A., Bernhofer, C., Bonal, D., Chen, J., Gianelle, D., Gobron, N., Kiely, G., Kutsch, W., Lasslop, G., Law, B. E., Lindroth, A., Merbold, L., Montagnani, L., Moors, E. J., Papale, D., Sottocornola, M., Vaccari, F., and Williams, C.: Global patterns of land-atmosphere fluxes of carbon dioxide, latent heat, and sensible heat derived from eddy covariance, satellite, and meteorological observations, Journal of Geophysical Research: Biogeosciences, 116, n/a–n/a, doi:10.1029/2010JG001566, http://dx.doi.org/10.1029/2010JG001566, g00J07, 2011.

Kim, D., Lee, M.-I., Jeong, S.-J., Im, J., Cha, D. H., and Lee, S.: Intercomparison of Terrestrial Carbon Fluxes and Carbon Use Efficiency Simulated by CMIP5 Earth System Models, Asia-Pacific Journal of Atmospheric Sciences, 54, 145–163, 2018.

Koven, C. D., Riley, W. J., Subin, Z. M., Tang, J. Y., Torn, M. S., Collins, W. D., Bonan, G. B., Lawrence, D. M., and Swenson, S. C.: The effect of vertically resolved soil biogeochemistry and alternate soil C and N models on C dynamics of CLM4, Biogeosciences, 10, 7109–7131, doi:10.5194/bg-10-7109-2013, http://www.biogeosciences.net/10/7109/2013/, 2013.

Lamarque, J.-F., Bond, T. C., Eyring, V., Granier, C., Heil, A., Klimont, Z., Lee, D., Liousse, C., Mieville, A., Owen, B., et al.: Historical (1850–2000) gridded anthropogenic and biomass burning emissions of reactive gases and aerosols: methodology and application, 2010.

Lamarque, J.-F., Shindell, D. T., Josse, B., Young, P. J., Cionni, I., Eyring, V., Bergmann, D., Cameron-Smith, P., Collins, W. J., Doherty, R., Dalsoren, S., Faluvegi, G., Folberth, G., Ghan, S. J., Horowitz, L. W., Lee, Y. H.,

https://doi.org/10.5194/gmd-2020-205
Preprint. Discussion started: 24 July 2020

MacKenzie, I. A., Nagashima, T., Naik, V., Plummer, D., Righi, M., Rumbold, S. T., Schulz, M., Skeie, R. B., Stevenson, D. S., Strode, S., Sudo, K., Szopa, S., Voulgarakis, A., and Zeng, G.: The Atmospheric Chemistry and Climate Model Intercomparison Project (ACCMIP): overview and description of models, simulations and climate diagnostics, Geoscientific Model Development, 6, 179–206, doi:10.5194/gmd-6-179-2013, https://www.geosci-model-dev.net/6/179/2013/, 2013.

Le Quéré, C., Andrew, R. M., Friedlingstein, P., Sitch, S., Hauck, J., Pongratz, J., Pickers, P. A., Korsbakken, J. I., Peters, G. P., Canadell, J. G., et al.: Global carbon budget 2018, Earth System Science Data (Online), 10, 2018.

LeBauer, D. S. and Treseder, K. K.: Nitrogen limitation of net primary productivity in terrestrial ecosystems is globally distributed, Ecology, 89, 371–379, doi:10.1890/06-2057.1, http://dx.doi.org/10.1890/06-2057.1, 2008.

Li, W., Ciais, P., Wang, Y., Yin, Y., Peng, S., Zhu, Z., Bastos, A., Yue, C., Ballantyne, A. P., Broquet, G., et al.: Recent changes in global photosynthesis and terrestrial ecosystem respiration constrained from multiple observations, Geophysical Research Letters, 2018.

Mercado, L. M., Huntingford, C., Gash, J. H., Cox, P. M., and Jogireddy, V.: Improving the representation of radiation interception and photosynthesis for climate model applications, Tellus B, 59, 553–565, 2007.

Mercado, L. M., Bellouin, N., Sitch, S., Boucher, O., Huntingford, C., Wild, M., and Cox, P. M.: Impact of changes in diffuse radiation on the global land carbon sink, Nature, 458, 1014–1017, 2009.

Meyerholt, J., Sickel, K., and Zaehle, S.: Ensemble projections elucidate effects of uncertainty in terrestrial nitrogen limitation on future carbon uptake, Global Change Biology, n/a, doi:10.1111/gcb.15114, https://onlinelibrary.wiley.com/doi/abs/10.1111/gcb.15114, 2020a.

Meyerholt, J., Sickel, K., and Zaehle, S.: Ensemble projections elucidate effects of uncertainty in terrestrial nitrogen limitation on future carbon uptake, Global Change Biology, 2020b.

Olson, D. M., Dinerstein, E., Wikramanayake, E. D., Burgess, N. D., Powell, G. V., Underwood, E. C., D'amico, J. A., Itoua, I., Strand, H. E., Morrison, J. C., et al.: Terrestrial Ecoregions of the World: A New Map of Life on Earth A new global map of terrestrial ecoregions provides an innovative tool for conserving biodiversity, BioScience, 51, 933–938, 2001.

Parton, W., Scurlock, J., Ojima, D., Gilmanov, T., Scholes, R., Schimel, D. S., Kirchner, T., Menaut, J.-C., Seastedt, T., Garcia Moya, E., et al.: Observations and modeling of biomass and soil organic matter dynamics for the grassland biome worldwide, Global biogeochemical cycles, 7, 785–809, 1993.

Post, W. M., Pastor, J., Zinke, P. J., and Stangenberger, A. G.: Global patterns of soil nitrogen storage, Nature, 317, 613, 1985.

Robertson, E., W. A. and Liddicoat, S.: A New Representation of Land-use in the JULES Land Surface Model, in prep.

Ruesch, A. and Gibbs, H. K.: New IPCC Tier-1 Global Biomass Carbon Map For the Year 2000.

Saatchi, S. S., Harris, N. L., Brown, S., Lefsky, M., Mitchard, E. T., Salas, W., Zutta, B. R., Buermann, W., Lewis, S. L., Hagen, S., et al.: Benchmark map of forest carbon stocks in tropical regions across three continents, Proceedings of the national academy of sciences, 108, 9899–9904, 2011.

Schlesinger, W. H.: Biogeochemistry: An Analysis of Global Change, Academic Press, San Diego, 2nd Edn., 1997.

https://doi.org/10.5194/gmd-2020-205
Preprint. Discussion started: 24 July 2020

Geoscientific Model Development Discussions

Sellar, A. A., Jones, C. G., Mulcahy, J. P., Tang, Y., Yool, A., Wiltshire, A., O'Connor, F. M., Stringer, M., Hill, R., Palmieri, J., Woodward, S., de Mora, L., Kuhlbrodt, T., Rumbold, S. T., Kelley, D. I., Ellis, R., Johnson, C. E., Walton, J., Abraham, N. L., Andrews, M. B., Andrews, T., Archibald, A. T., Berthou, S., Burke, E., Blockley, E., Carslaw, K., Dalvi, M., Edwards, J., Folberth, G. A., Gedney, N., Griffiths, P. T., Harper, A. B., Hendry, M. A., Hewitt, A. J., Johnson, B., Jones, A., Jones, C. D., Keeble, J., Liddicoat, S., Morgenstern, O., Parker, R. J., Predoi, V., Robertson, E., Siahaan, A., Smith, R. S., Swaminathan, R., Woodhouse, M. T., Zeng, G., and Zerroukat, M.: UKESM1: Description and Evaluation of the U.K. Earth System Model, Journal of Advances in Modeling Earth Systems, 11, 4513–4558, doi:10.1029/2019MS001739, https://agupubs.onlinelibrary.wiley.com/doi/abs/10.1029/2019MS001739, 2019.

Sitch, S., Friedlingstein, P., Gruber, N., Jones, S., Murray-Tortarolo, G., Ahlström, A., Doney, S. C., Graven, H., Heinze, C., Huntingford, C., et al.: Recent trends and drivers of regional sources and sinks of carbon dioxide, Biogeosciences, 12, 653–679, 2015.

Smith, B., Warlind, D., Arneth, A., Hickler, T., Leadley, P., Siltberg, J., and Zaehle, S.: Implications of incorporating N cycling and N limitations on primary production in an individual-based dynamic vegetation model, Biogeosciences, 11, 2027–2054, 2014.

Taylor, K. E., Stouffer, R. J., and Meehl, G. A.: An overview of CMIP5 and the experiment design, Bulletin of the American Meteorological Society, 93, 485–498, 2012.

Thomas, R., Bonan, G., and Goodale, C.: Insights into mechanisms governing forest carbon response to nitrogen deposition: a model–data comparison using observed responses to nitrogen addition, Biogeosciences, 10, 3869–3887, 2013.

von Bloh, W., Schaphoff, S., Müller, C., Rolinski, S., Waha, K., and Zaehle, S.: Implementing the Nitrogen cycle into the dynamic global vegetation, hydrology and crop growth model LPJmL (version 5), Geoscientific Model Development, 2018.

Wania, R., Meissner, K., Eby, M., Arora, V., Ross, I., and Weaver, A.: Carbon-nitrogen feedbacks in the UVic ESCM, Geoscientific Model Development, 5, 1137–1160, 2012.

Weintraub, M. N. and Schimel, J. P.: Nitrogen Cycling and the Spread of Shrubs Control Changes in the Carbon Balance of Arctic Tundra Ecosystems, BioScience, 55, 408–415, doi:10.1641/0006-3568(2005)055[0408:NCATSO]2.0.CO;2, https://doi.org/10.1641/0006-3568(2005)055[0408:NCATSO]2.0.CO;2, 2005.

Wenzel, S., Cox, P. M., Eyring, V., and Friedlingstein, P.: Projected land photosynthesis constrained by changes in the seasonal cycle of atmospheric CO 2, Nature, 538, 499–501, 2016.

Wiltshire, A. J., Duran Rojas, M. C., Edwards, J. M., Gedney, N., Harper, A. B., Hartley, A. J., Hendry, M. A., Robertson, E., and Smout-Day, K.: JULES-GL7: the Global Land configuration of the Joint UK Land Environment Simulator version 7.0 and 7.2, Geoscientific Model Development, 13, 483–505, doi:10.5194/gmd-13-483-2020, https://www.geosci-model-dev.net/13/483/2020/, 2020.

Xu-Ri and Prentice, I. C.: Terrestrial nitrogen cycle simulation with a dynamic global vegetation model, Global Change Biology, 14, 1745–1764, doi:10.1111/j.1365-2486.2008.01625.x, http://dx.doi.org/10.1111/j.1365-2486.2008.01625.x, 2008.

https://doi.org/10.5194/gmd-2020-205
Preprint. Discussion started: 24 July 2020

Geoscientific Model Development Discussions

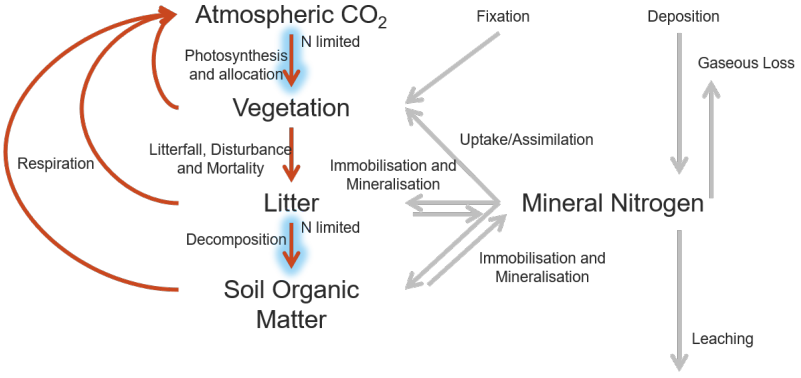

Figure 1. Schematic of the nitrogen cycling within the JULES-CN model. Carbon fluxes are shown in red, Nitrogen fluxes in grey. Nitrogen limited carbon fluxes are highlighted in blue.

Zaehle, S.: Terrestrial nitrogen–carbon cycle interactions at the global scale, Philosophical Transactions of the Royal Society of London B: Biological Sciences, 368, doi:10.1098/rstb.2013.0125, http://rstb.royalsocietypublishing.org/content/368/1621/20130125, 2013a.

Zaehle, S.: Terrestrial nitrogen–carbon cycle interactions at the global scale, Philosophical Transactions of the Royal Society B: Biological Sciences, 368, 20130 125, 2013b.

Zaehle, S. and Dalmonech, D.: Carbon–nitrogen interactions on land at global scales: current understanding in modelling climate biosphere feedbacks, Current Opinion in Environmental Sustainability, 3, 311–320, 2011.

Zaehle, S. and Friend, A.: Carbon and nitrogen cycle dynamics in the O-CN land surface model: 1. Model description, site-scale evaluation, and sensitivity to parameter estimates, Global Biogeochemical Cycles, 24, 2010.

Zaehle, S., Medlyn, B. E., De Kauwe, M. G., Walker, A. P., Dietze, M. C., Hickler, T., Luo, Y., Wang, Y.-P., El-Masri, B., Thornton, P., Jain, A., Wang, S., Warlind, D., Weng, E., Parton, W., Iversen, C. M., Gallet-Budynek, A., McCarthy, H., Finzi, A., Hanson, P. J., Prentice, I. C., Oren, R., and Norby, R. J.: Evaluation of 11 terrestrial carbon–nitrogen cycle models against observations from two temperate Free-Air CO2 Enrichment studies, New Phytologist, 202, 803–822, doi:10.1111/nph.12697, http://dx.doi.org/10.1111/nph.12697, 2013-16358, 2014.

Zhao, M. and Running, S. W.: Drought-induced reduction in global terrestrial net primary production from 2000 through 2009, science, 329, 940–943, 2010.

Figures

https://doi.org/10.5194/gmd-2020-205
Preprint. Discussion started: 24 July 2020

Geoscientific Model Development Discussions
Open Access
EGU

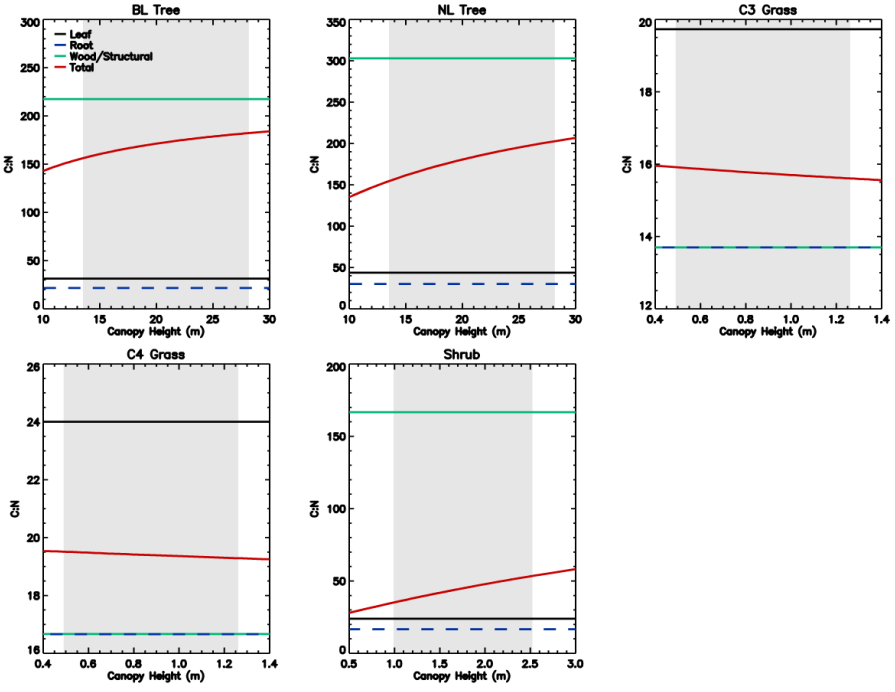

Figure 2. Stochiometry of the vegetation nitrogen pools as a function of canopy height for individual PFTs at full leaf. Leaf N concentration are defined at the canopy level and are approximately % higher than those for the top leaf. The grey region shows the defined range of canopy height within the model.

https://doi.org/10.5194/gmd-2020-205
Preprint. Discussion started: 24 July 2020

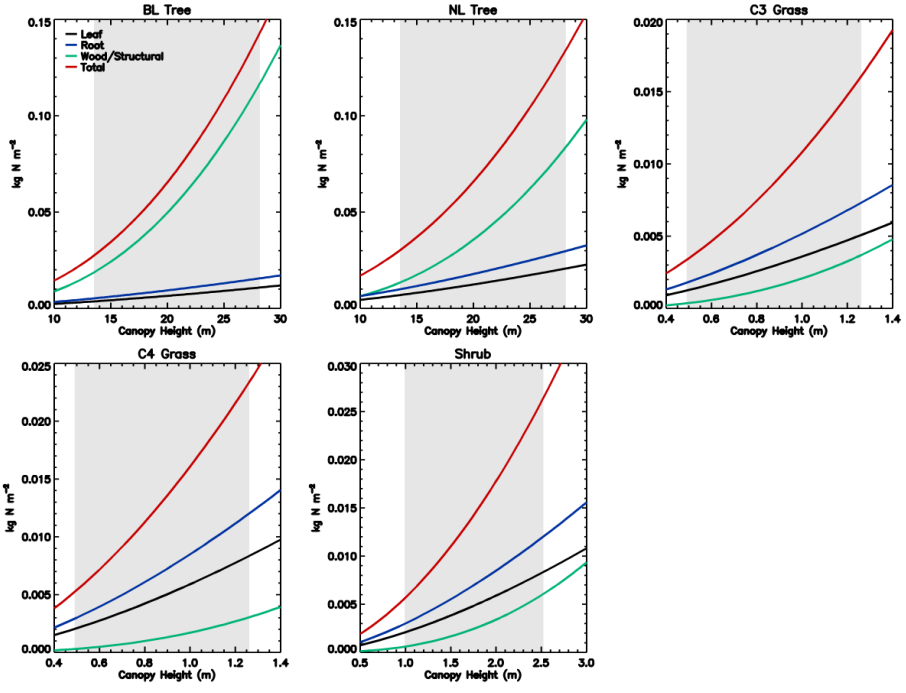

Figure 3. Total vegetation and component nitrogen pools as a function of canopy height for individual PFTs at full leaf. The grey region shows the defined range of canopy height within the model.

https://doi.org/10.5194/gmd-2020-205
Preprint. Discussion started: 24 July 2020

Geoscientific Model Development
Discussions
Open Access
EGU

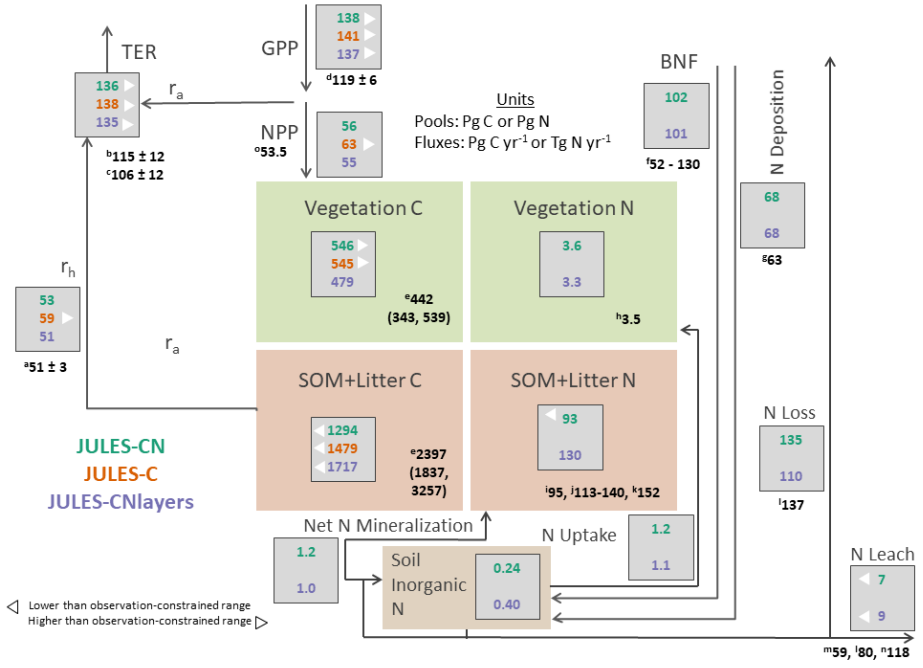

Figure 4. Carbon and nitrogen stocks and fluxes for JULES-CN, JULES-C, and JULES-CN$_{layered}$ for the period 19960-2005 (after Davies-Barnard et al. (2020)). C = Carbon; N = Nitrogen; r_h = Heterotrophic respiration; r_a = Autotrophic respiration; TER = Total ecosystem respiration; GPP = Gross primary productivity; SOM = Soil organic matter; BNF = Biological nitrogen fixation. The black numbers are the observational-constrained values from the literature: (a) Heterotrophic respiration: Hashimoto et al. (2015); (b) TER: Li et al. (2018); (c) TER: Ballantyne et al. (2017); (d) GPP: Jung et al. (2011); (e) Vegetation carbon and SOM+litter carbon: Carvalhais et al. (2014); (f) BNF Davies-Barnard and Friedlingstein (2020); (g) N deposition: Lamarque et al. (2010); (h) Vegetation nitrogen: Schlesinger (1997); (i) soil organic nitrogen: Post et al. (1985); (j) soil organic nitrogen: Batjes (2014); (k) soil organic nitrogen: Group (2000); (l) nitrogen losses including nitrogen leaching: Gruber and Galloway (2008); (m) nitrogen leaching: Boyer et al. (2006); (n) nitrogen leaching: Galloway et al. (2004); and (o) NPP: Zhao and Running (2010).

https://doi.org/10.5194/gmd-2020-205
Preprint. Discussion started: 24 July 2020

Geoscientific Model Development Discussions
Open Access
EGU

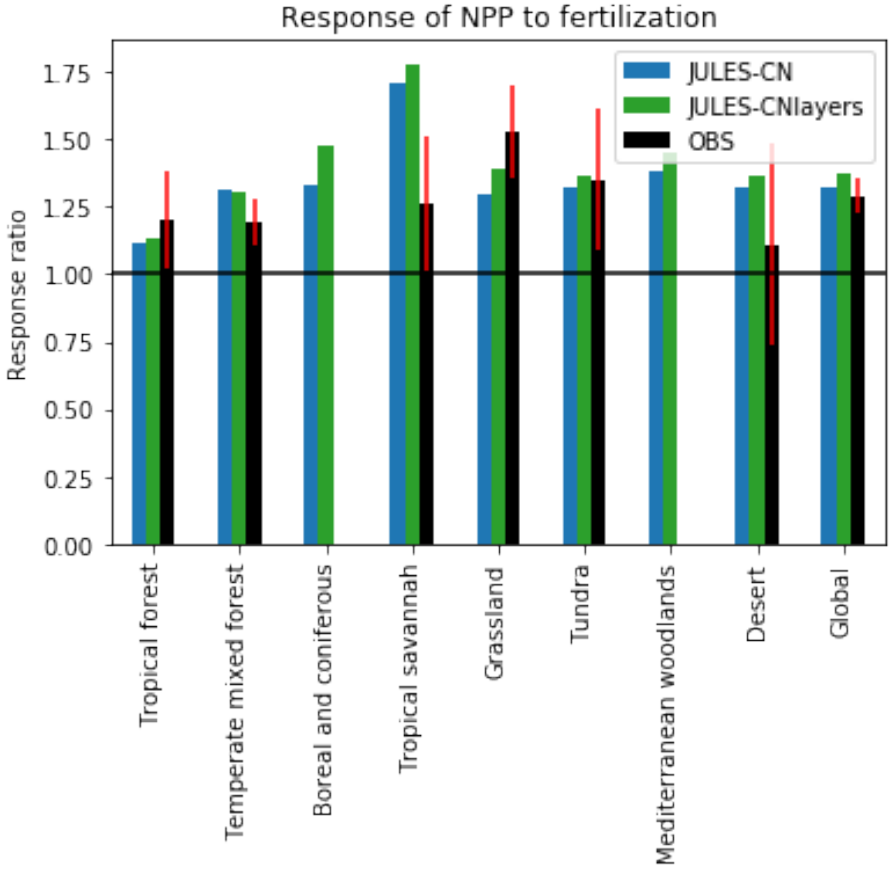

Figure 5. The response ratio, is the ratio of net primary productivity produced when fully fertilised (NPP_{pot}) compared with that achieved for the natural state (NPP). A value greater than one means that the addition of nitrogen will enhance NPP. In the model the globe is split into biomes representing the following - TF: Tropical Forests; MF: Temperate Mixed Forests; BF: Boreal Forests; TS: Tropical Savannah; TG: Temperate Grasslands; TU: Tundra; MED: Mediterranean Woodlands; and D: Deserts. The different biomes were characterised by Harper et al. (2018) based the 14 World Wildlife Fund terrestrial ecoregions (Olson et al., 2001). The mean of JULES-CN and JULES-CN$_{layers}$ are shown for the period 1996-2005. The observational constraint is taken from Table 1 in LeBauer and Treseder (2008), with the black bars showing the mean and the red lines the uncertainty.

https://doi.org/10.5194/gmd-2020-205
Preprint. Discussion started: 24 July 2020

Geoscientific Model Development Discussions
Open Access
EGU

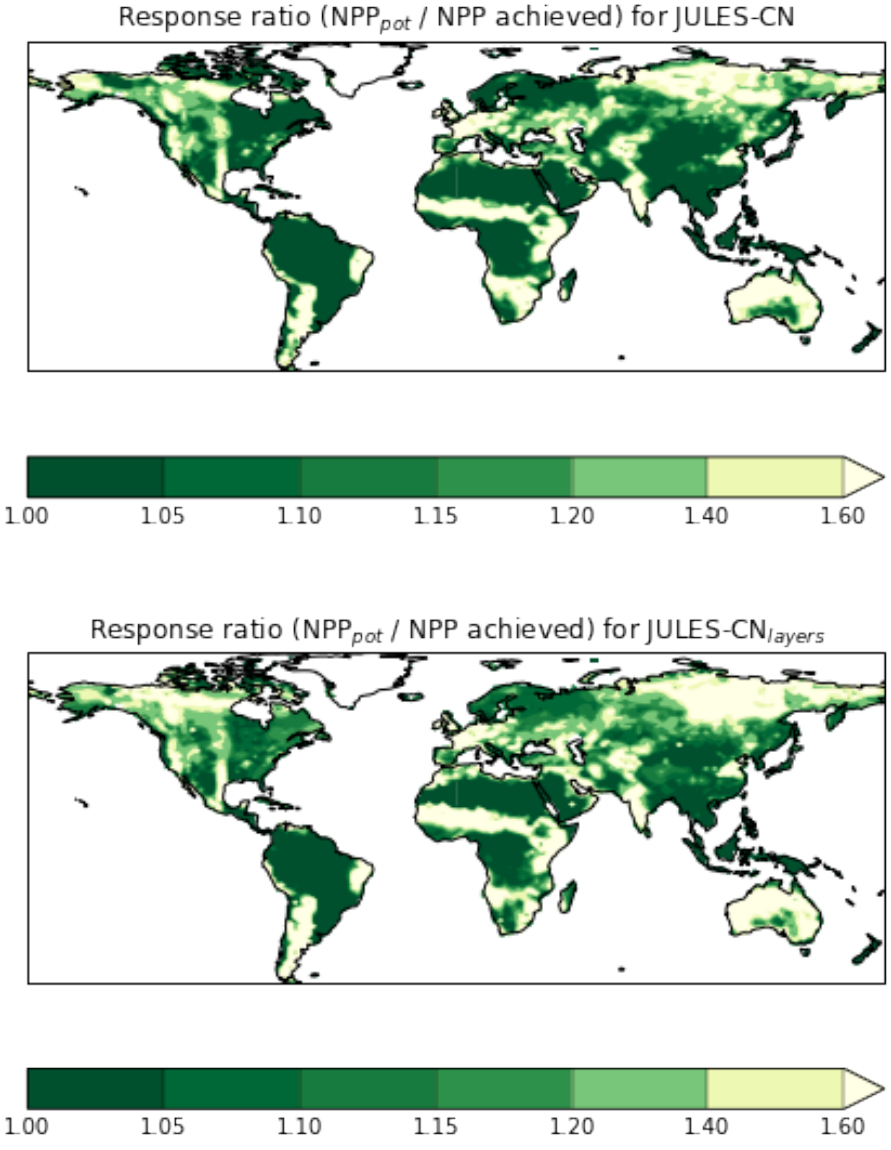

Figure 6. The spatial distribution of the response ratio defined as the potential NPP (NPP$_{pot}$) when fully fertilised as a fraction of the NPP achieved in the natural state for (a) JULES-CN, and (b) JULES-CN$_{layered}$. This is the spatial distribution of the metric shown in 5.

https://doi.org/10.5194/gmd-2020-205
Preprint. Discussion started: 24 July 2020

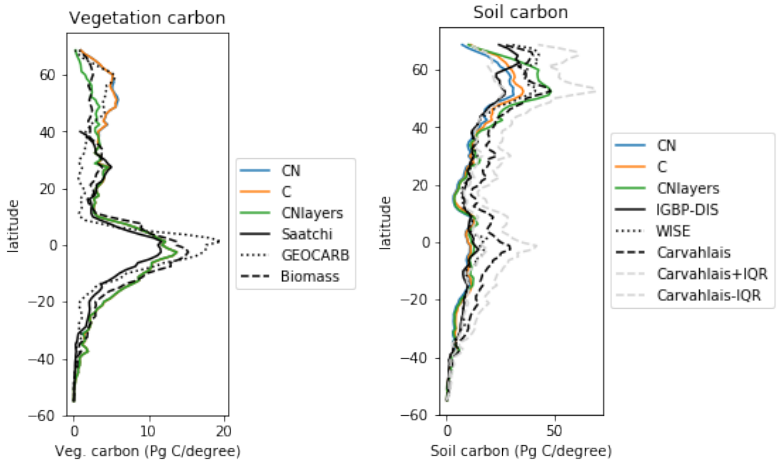

Figure 7. Zonal total values of soil and vegetation carbon for JULES-C, JULES-CN and JULES-CN$_{layered}$ simulations for the period 1996-2005 in Pg C / degree of latitude. For the vegetation carbon the observational-based constrains are Saatchi: Saatchi et al. (2011); GEOCARB: Avitabile et al. (2016); and Biomass: Ruesch and Gibbs. The observatioal-based constrainst for the soil carbon are IGBP-DIS: Group (2000); WISE: Batjes (2016); and Carvahlais: Carvalhais et al. (2014).

https://doi.org/10.5194/gmd-2020-205
Preprint. Discussion started: 24 July 2020

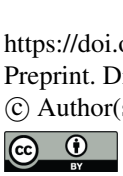

Geoscientific Model Development Discussions
Open Access
EGU

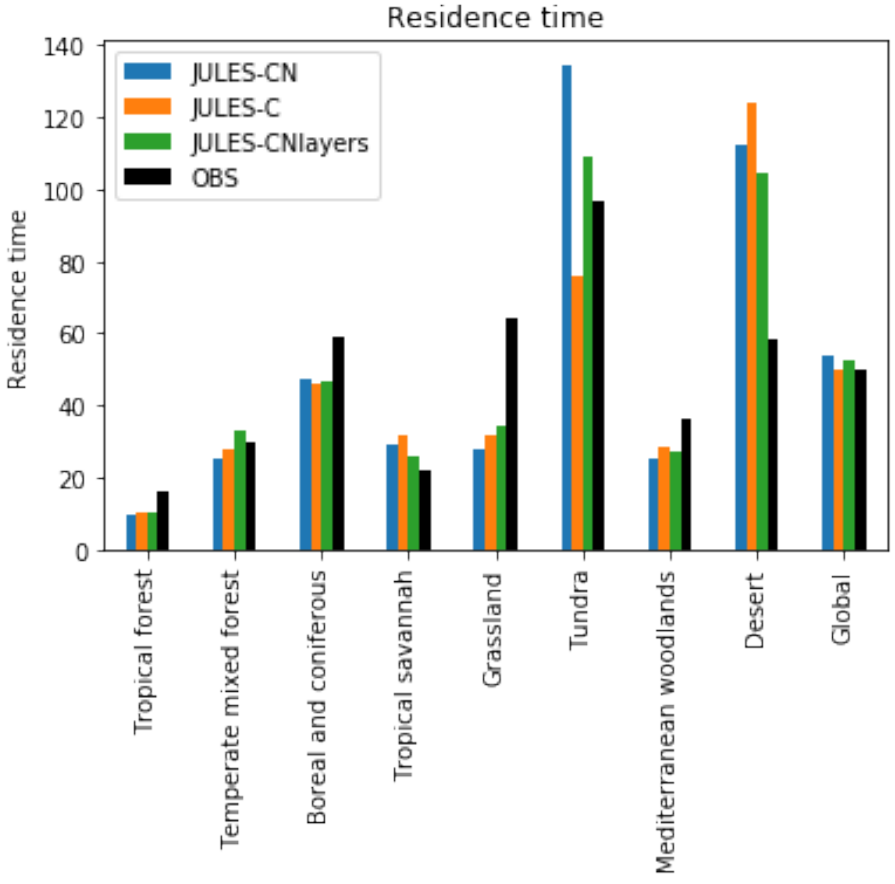

Figure 8. Biome-based ecosystem turnover times calculated on a grid-cell by grid-cell basis then aggregated temporally to biome level. JULES-C, JULES-CN and JULES-CN$_{layers}$ are shown for the period 1996-2005. The biomes are discussed in more detail in Figure 5. The observations are derived from the Carvalhais et al. (2014) global data set.

https://doi.org/10.5194/gmd-2020-205
Preprint. Discussion started: 24 July 2020

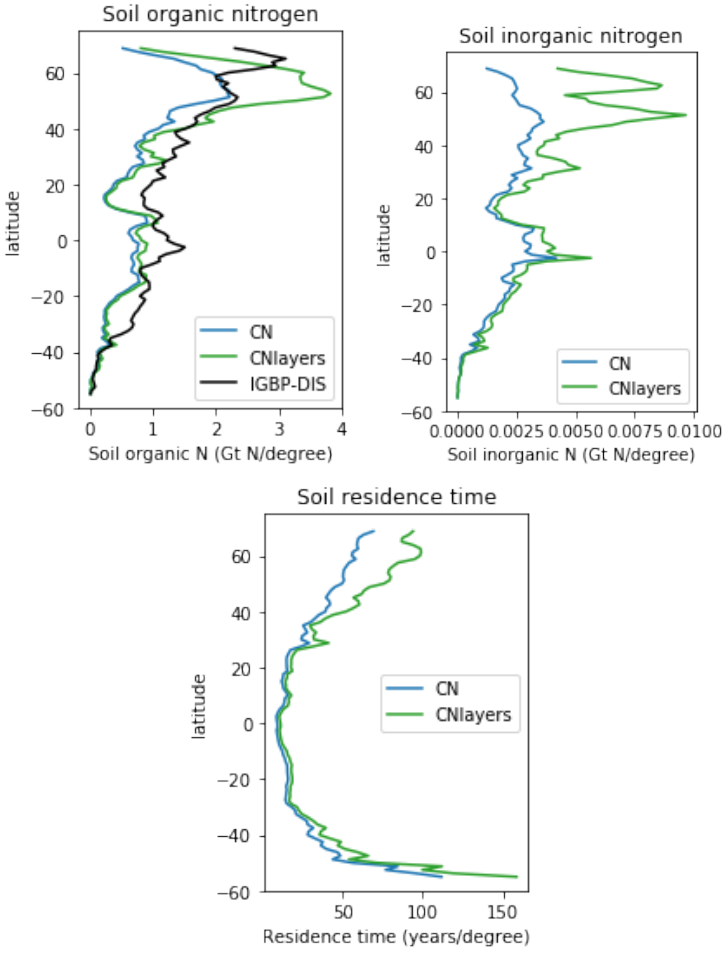

Figure 9. The zonal total soil organic and inorganic nitrogen stocks in Pg N / degree of latitude. The organic nitrogen stocks are from Group (2000). Also shown are the residence times as the ratio of total soil organic carbon divided by the soil respiration.

https://doi.org/10.5194/gmd-2020-205
Preprint. Discussion started: 24 July 2020

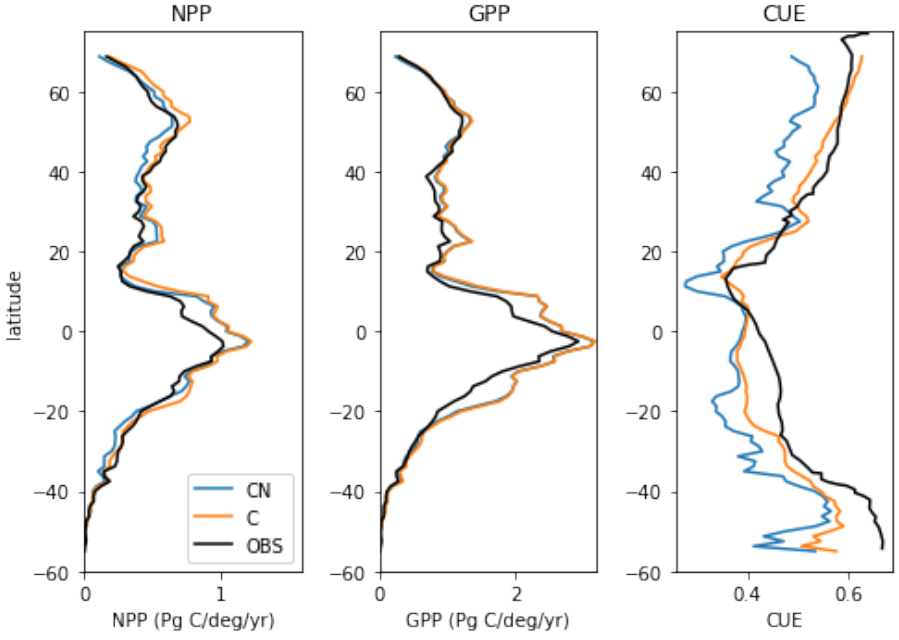

Figure 10. Zonal total values of net primary productivity (NPP) and gross primary productivity (GPP) for JULES-C and JULES-CN simulations for the period 1996-2005 in Pg C / degree of latitude / year. The observational-constraint for NPP is from MODIS (Zhao and Running, 2010) and that for GPP is from Jung et al. (2011). The zonal mean carbon use efficiency (CUE = NPP/GPP) is also shown. The CUE observational constraint was digitised from Kim et al. (2018).

https://doi.org/10.5194/gmd-2020-205
Preprint. Discussion started: 24 July 2020

Geoscientific Model Development Discussions
Open Access
EGU

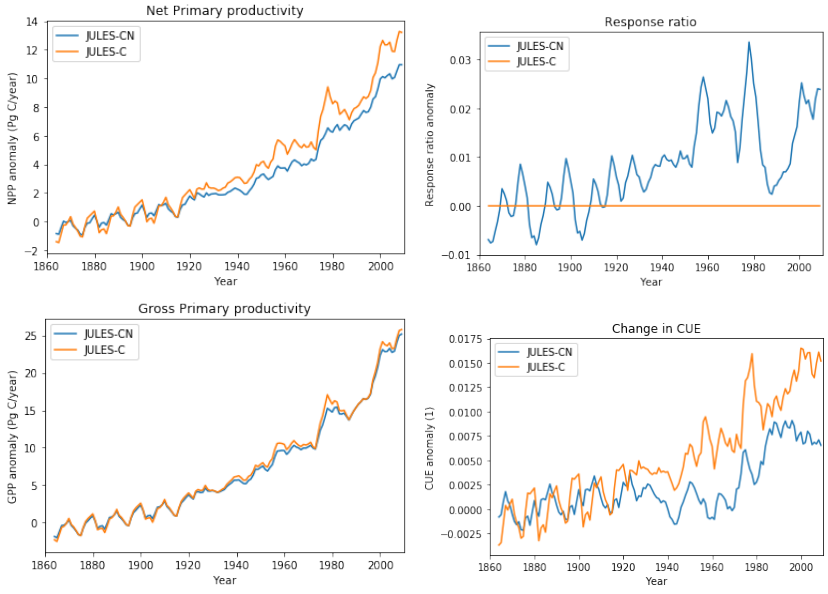

Figure 11. Change in NPP, the response ratio (potential NPP / NPP acheived), GPP and CUE for JULES-CN and JULES-C over the historical period with respect to the multi-annual mean period of 1860-1899.

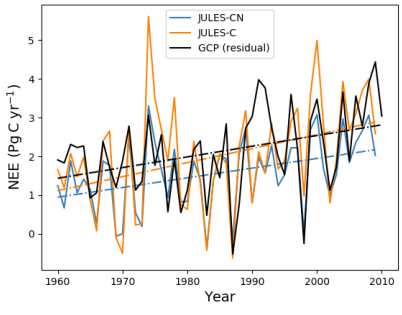

Figure 12. Evaluation of global annual mean NEE from JULES-C and JULES-CN, against observation based estimates from GCP (Friedlingstein et al. 2019), over the period from 1960 to 2009 inclusive. Positive values represent the land surface as a net sink of carbon.